NAVAL POSTGRADUATE SCHOOL

MONTEREY, CALIFORNIA

THESIS

HORIZONTAL WIND VEERING AND BACKING NEAR THE COASTLINE WITHIN MONTEREY BAY

by

Ian P. Jenstrom

June 2023

Thesis Advisor: James H. MacMahan
Second Reader: Edward B. Thornton

THIS PAGE INTENTIONALLY LEFT BLANK

REPORT DOCUMENTATION PAGE	*Form Approved OMB No. 0704-0188*

1. AGENCY USE ONLY *(Leave blank)*	**2. REPORT DATE** June 2023	**3. REPORT TYPE AND DATES COVERED** Master's thesis

4. TITLE AND SUBTITLE
HORIZONTAL WIND VEERING AND BACKING NEAR THE COASTLINE WITHIN MONTEREY BAY

5. FUNDING NUMBERS

6. AUTHOR(S) Ian P. Jenstrom

7. PERFORMING ORGANIZATION NAME(S) AND ADDRESS(ES)
Naval Postgraduate School
Monterey, CA 93943-5000

8. PERFORMING ORGANIZATION REPORT NUMBER

9. SPONSORING / MONITORING AGENCY NAME(S) AND ADDRESS(ES)
N/A

10. SPONSORING / MONITORING AGENCY REPORT NUMBER

11. SUPPLEMENTARY NOTES The views expressed in this thesis are those of the author and do not reflect the official policy or position of the Department of Defense or the U.S. Government.

12a. DISTRIBUTION / AVAILABILITY STATEMENT
Approved for public release. Distribution is unlimited.

12b. DISTRIBUTION CODE
A

13. ABSTRACT (maximum 200 words)

A three-phase field experiment was conducted in and around Monterey Bay, CA, in 2021 and 2022 using a combination of 18 moored air-sea spar buoys to describe horizontal wind veering along the coastal ocean. Hourly-mean wind speeds and directions were collected from anemometers at 4 m heights. Phase 1 (June-July 2021) focused predominantly on cross-shore winds within southern Monterey Bay. Phase 2 (August 2021) focused on winds around the complex headland of Monterey Peninsula. Phase 3 (August 2022) examined alongshore winds off Santa Cruz. Due to the persistent diurnal sea breeze pattern within the bay, canonical days were analyzed at each buoy to understand changes in wind speed and direction. Three cross-shore arrays were used to analyze topographic influences on surface wind behavior. All three arrays found winds veering and backing with decreasing distance to shore due to the presence of land and the differential roughness influencing the wind speed. The Bellamy method was used to compute Differential Kinematic Properties (DKPs) of vorticity, divergence, shear and stretch by using triangles with corners delineated by buoy locations. Twelve triangle centers were chosen for both Phase 2 and Phase 3. The response to wind veering and backing by the coastal topography induce cross- and alongshore gradients in the wind that can be described and quantified with DKPs.

14. SUBJECT TERMS
Differential Kinematic Properties, coast, boundaries, divergence, vorticity, shear, stretch, Monterey Bay, Santa Cruz, wind flow, ocean wind, coastal ocean, surface winds, wind veering, wind backing, wind turning

15. NUMBER OF PAGES
55

16. PRICE CODE

17. SECURITY CLASSIFICATION OF REPORT	**18. SECURITY CLASSIFICATION OF THIS PAGE**	**19. SECURITY CLASSIFICATION OF ABSTRACT**	**20. LIMITATION OF ABSTRACT**
Unclassified	Unclassified	Unclassified	UU

NSN 7540-01-280-5500

Standard Form 298 (Rev. 2-89)
Prescribed by ANSI Std. 239-18

THIS PAGE INTENTIONALLY LEFT BLANK

Approved for public release. Distribution is unlimited.

HORIZONTAL WIND VEERING AND BACKING NEAR THE COASTLINE WITHIN MONTEREY BAY

Ian P. Jenstrom
Lieutenant, United States Navy
BS, University of South Carolina, Columbia, 2016

Submitted in partial fulfillment of the
requirements for the degree of

MASTER OF SCIENCE IN METEOROLOGY AND PHYSICAL OCEANOGRAPHY

from the

NAVAL POSTGRADUATE SCHOOL
June 2023

Approved by: James H. MacMahan
Advisor

Edward B. Thornton
Second Reader

Peter C. Chu
Chair, Department of Oceanography

THIS PAGE INTENTIONALLY LEFT BLANK

ABSTRACT

A three-phase field experiment was conducted in and around Monterey Bay, CA, in 2021 and 2022 using a combination of 18 moored air-sea spar buoys to describe horizontal wind veering along the coastal ocean. Hourly-mean wind speeds and directions were collected from anemometers at 4 m heights. Phase 1 (June-July 2021) focused predominantly on cross-shore winds within southern Monterey Bay. Phase 2 (August 2021) focused on winds around the complex headland of Monterey Peninsula. Phase 3 (August 2022) examined alongshore winds off Santa Cruz. Due to the persistent diurnal sea breeze pattern within the bay, canonical days were analyzed at each buoy to understand changes in wind speed and direction. Three cross-shore arrays were used to analyze topographic influences on surface wind behavior. All three arrays found winds veering and backing with decreasing distance to shore due to the presence of land and the differential roughness influencing the wind speed. The Bellamy method was used to compute Differential Kinematic Properties (DKPs) of vorticity, divergence, shear and stretch by using triangles with corners delineated by buoy locations. Twelve triangle centers were chosen for both Phase 2 and Phase 3. The response to wind veering and backing by the coastal topography induce cross- and alongshore gradients in the wind that can be described and quantified with DKPs.

THIS PAGE INTENTIONALLY LEFT BLANK

TABLE OF CONTENTS

THIS PAGE INTENTIONALLY LEFT BLANK

LIST OF FIGURES

THIS PAGE INTENTIONALLY LEFT BLANK

LIST OF ACRONYMS AND ABBREVIATIONS

ASIS	Air Sea Interaction Spar (buoy)
DKP	Differential Kinematic Property
IMU	Inertial Motion Unit
ISPAR	Inner-shelf Spar (buoy)
LSB	Land Sea Breeze
NOAA	National Oceanic Atmospheric Administration
OWn	normalized Okubo-Weiss parameter

THIS PAGE INTENTIONALLY LEFT BLANK

I. INTRODUCTION

The changes in wind behavior due to topography plays an important role in the air-sea interaction of the coastal zone. Coastal wind veering and backing, the shifting in wind direction as wind flows over the sea/land interface, has been described by sailors and forecast handbooks for years but has yet to be quantified due to difficulty obtaining observations in the coastal zone (Brettle 1994; Steele et al. 2014). Additionally, coastal topography and coastal wind veering and backing influence wind differential kinematic properties (DKP) of vorticity, divergence, shear, and stretch.

Past research of onshore coastal wind veering and backing is scarce due to the complexity of obtaining synchronous wind measurements at various locations in the coastal zone from buoys deployed in a shallow water wave environment. Olufsen et al. (1985) describe a critical wind angle of 20 degrees from normal to the coast, where frictional convergence of surface winds can cause upward motion and lead to precipitation. Savijärvi (2004) modeled how coastal friction causes changes in wind speeds using land observations from a previous experiment along the North Sea Dutch coast (Kudryavtsev et al. 2000) over scales 1–10km. When winds were onshore from a cold sea to a warm coast (similar to Monterey Bay), model results displayed strong and steady winds up to the sea/land interface with some backing of the cross-isobar angle 10 to 30km out to sea and reduced wind speed and veering of the cross-isobar angle over land (Savijärvi 2004). In another experiment, anemometers mounted on catamarans ranging in heights from 5 to 28m and a land-based sodar deployed within Quiberon Bay, France, during daytime hours were used to analyze Land Sea Breeze (LSB) wind flow regimes of pure, corkscrew, and backdoor (Steele et al. 2014) for sailing purposes (Mestayer et al. 2018).

The dominant weather pattern seen in Monterey Bay, CA, is the Land Sea Breeze (LSB). Numerous studies have analyzed the LSB phenomenon caused by differential heating of the land and sea creating differences in air pressure leading to onshore and offshore winds (Henrickson and MacMahan 2009; Steele et al. 2014; Abbs and Physick 1992; Miller et al. 2003; Darby and Banta 2002; Savijärvi 2004; Banta et al. 1993). A reduction of the LSB can occur when clouds are present leading to reduced or delayed land

heating during the day and a smaller pressure gradient between the land and sea (Savijärvi 2004). The LSB of Monterey Bay largely flows in the east-west direction. The Land Sea Breeze Experiment (LASBEX) placed a Doppler Lidar at Moss Landing (center of Monterey Bay) to analyze the horizontal and vertical structure of the LSB and its interaction with the coastal mountains through observations and models (Darby and Banta 2002). The strongest winds of the LSB were seen within the Salinas Valley, with blocking effects of the coastal mountain range enhancing the depth of the LSB (Darby and Banta 2002). Other observations identify a south-to-north pressure gradient maximized in the afternoon and evening between Monterey and Santa Cruz, driving flow down the gradient from Monterey to Santa Cruz (Archer and Jacobson 2005). Prevailing winds within Monterey Bay are from the northwest due to the subtropical North Pacific High-pressure system usually present off the California coast (Darby and Banta 2002). This prevailing wind flow, along with the daily LSB, has been observed to cause upwelling, bringing cold waters to the surface and enhancing the sea/land temperature gradient (Darby and Banta 2002) (Woodson et al. 2007).

Direct measurements of DKPs over the coastal ocean environment are difficult to obtain due to the necessity of arrays of spatial measurements, which can be challenging to obtain over the ocean. Most ocean wind flow research has examined vorticity generation on the lee side of an object through satellite observations or modeling (Smith et al. 1996; Gao et al. 2022; Pullen et al. 2017). Other research into DKPs has analyzed ocean currents flowing around islands and headlands (Rudnick et al. 2019; Kovatch et al. 2021; Dukhovskoy et al. 2017). DKPs were measured in the coastal environment using data from land weather stations and three NOAA buoys to create a high-resolution model to understand vorticity generation and advection within Monterey Bay, specifically examining the phenomenon of the Santa Cruz eddy, a cyclonic circulation within the boundary layer formed southeast of Santa Cruz (Tseng et al. 2011). Model results in northern Monterey Bay found positive vorticity (counterclockwise rotation) generated from the friction of positive coastal wind shear (faster winds moving over the ocean to the south and slower winds over land to the north) due to differences in surface roughness along with observations of wind convergence flow blocking owing to the northerly winds

encountering the Santa Cruz Mountains, validating previous observations (Archer and Jacobson 2005; Tseng et al. 2011). Another model observed frictional effects from convergence at coastlines creating secondary mesoscale circulations leading to precipitation (Roeloffzen et al. 1985). Savijärvi (2004) used a high-resolution (1 km) model simulating largescale wind flow regimes (excluding LSB) to understand how coast roughness effects wind flow direction, speed, flow convergence and divergence, and vertical stability.

This paper uses arrays of specially designed wind spar buoys deployed in arrays within the coastal zone in and around Monterey Bay, CA, to quantify the wind flow dynamics of ocean surface wind veering and backing from offshore to shore, along with the spatial and temporal changes in DKP. The methods section next describes how the wind data were obtained, and the steps taken for filtering and processing the data used to analyze wind veering and backing, and DKPs. The results section describes the three phases of the experiment and considers wind veering and backing and vorticity generation within the coastal zone. The discussion section attempts to sync ocean surface wind veering and backing and DKPs as it applies to the daily LSB and synoptic flow.

THIS PAGE INTENTIONALLY LEFT BLANK

II. METHODS

Data were acquired using sonic anemometers collocated with inertial motion (IMU) units to correct for motion, fixed at an elevation 4m above the water surface on two types of moored buoys: Naval Postgraduate School Inner-shelf Spar (ISPAR) buoys and Miami University Air Sea Interaction Spar (ASIS) buoys (Figure 1). The experiment consisted of three phases: Phase 1 (June to July 2021) between the Monterey Peninsula, CA, and Moss Landing, CA; Phase 2 (August 2021) around the Monterey Peninsula, CA; and Phase 3 (August 2022) off Santa Cruz, CA. A total of 10 ISPAR buoys and 8 ASIS buoys were available for each experiment. Figures 2 through 4 show the locations and names of the buoys used in relation to Monterey Bay for each Phase. ASIS buoys were generally located farther offshore than the ISPAR buoys placed in waters ranging from 7m to 30m. ASIS buoys were also deployed for Phase 3, but wind data were not available before the writing of this paper.

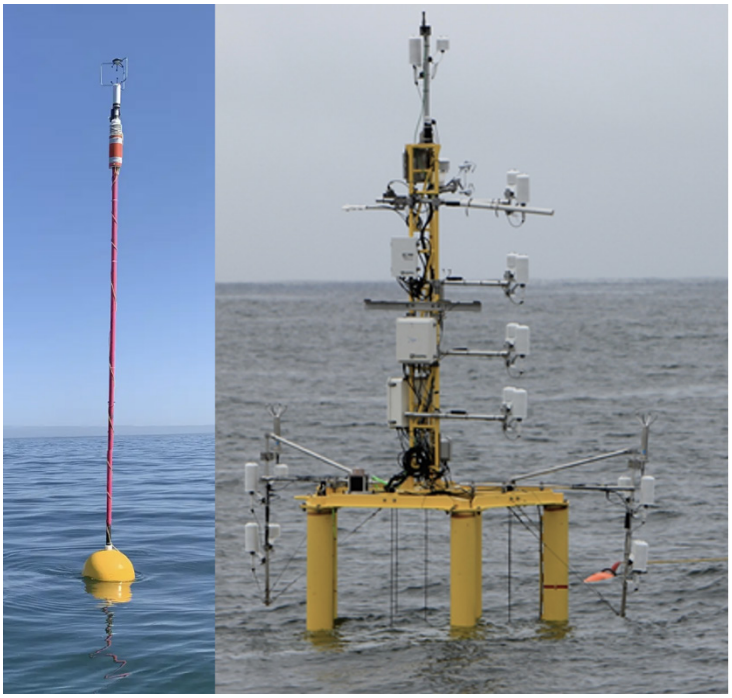

(Left) ISPAR buoy with sonic anemometer and IMU at 4m height. (Right) ASIS buoy with sonic anemometer and IMU at 4m height, along with other sensors.

Figure 1. Ocean Sensing Buoys

(Left) ISPAR buoys located off Del Monte Beach, Sand City, and Marina. (Right) ASIS buoys located farther offshore from Marina and Moss Landing.

Figure 2. Phase 1 Buoy Locations

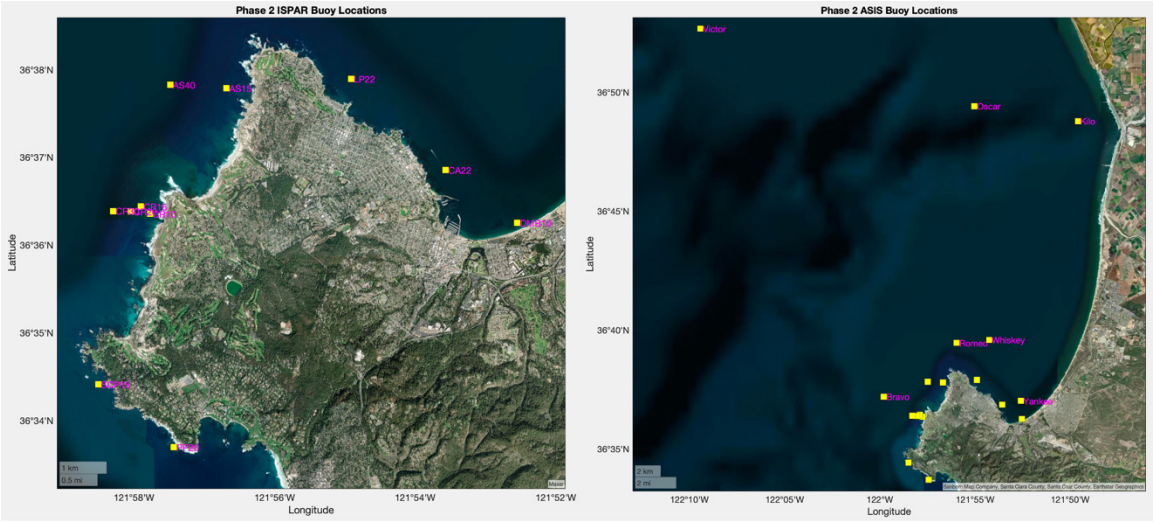

(Left) ISPAR buoys surrounding the Monterey Peninsula coast. (Right) ASIS buoys surrounding the Monterey Peninsula and within the bay center.

Figure 3. Phase 2 Buoy Locations

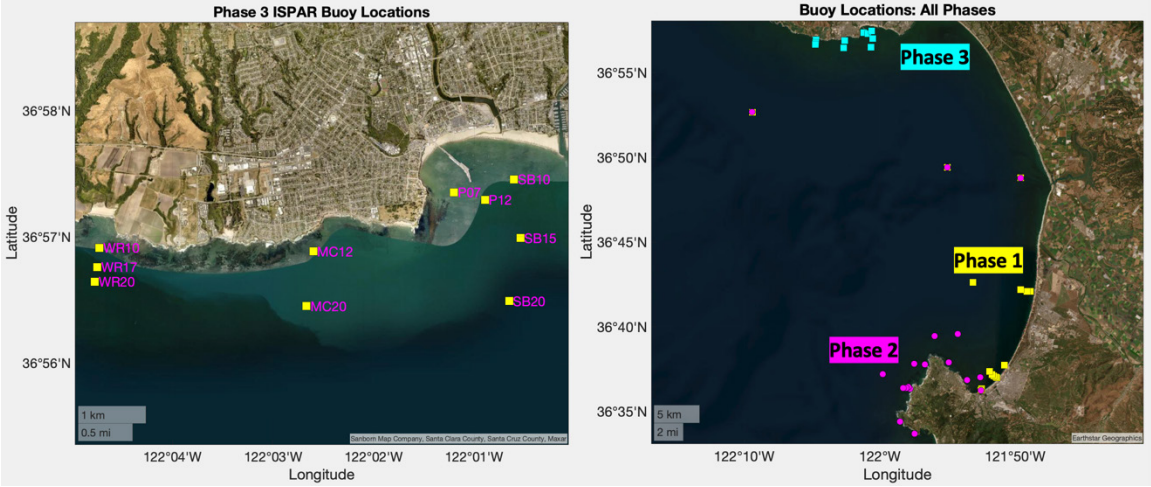

(Left) Phase 3 ISPAR buoy locations within and west of Santa Cruz harbor. (Right) Buoy locations for all phases in relation to each other. Phase 1: Yellow squares. Phase 2: magenta circles (overlapping ASIS buoys for Phases 1 & 2 within the center of Monterey Bay). Phase 3: blue squares.

Figure 4. Buoy Locations for All Phases

The coastline between Monterey and Moss Landing (halfway point of Monterey Bay) consists of sandy beaches and sand dunes. The Monterey Peninsula from Monterey south around to Carmel is composed of rocky coastlines with small, interspersed pocket beaches. The western Santa Cruz coastline is composed primarily of cliffs greater than 4m until reaching Santa Cruz harbor, where the coast becomes a sandy beach.

Wind and location data were collected during the first 30min of each hour and averaged (referred to as hourly averages) for each buoy. Changes in surface wind velocity over a day are examined using a wind velocity canonical day created by averaging wind velocity for each hour of the day at each buoy for each phase. The LSB is noticeable at all buoys within all phases, observed by the increase in wind speed in the afternoon and evening, and lower wind speed at night and early morning. Figure 5 shows the velocity canonical day for a selection of buoys from all three phases, displaying a LSB over space and time.

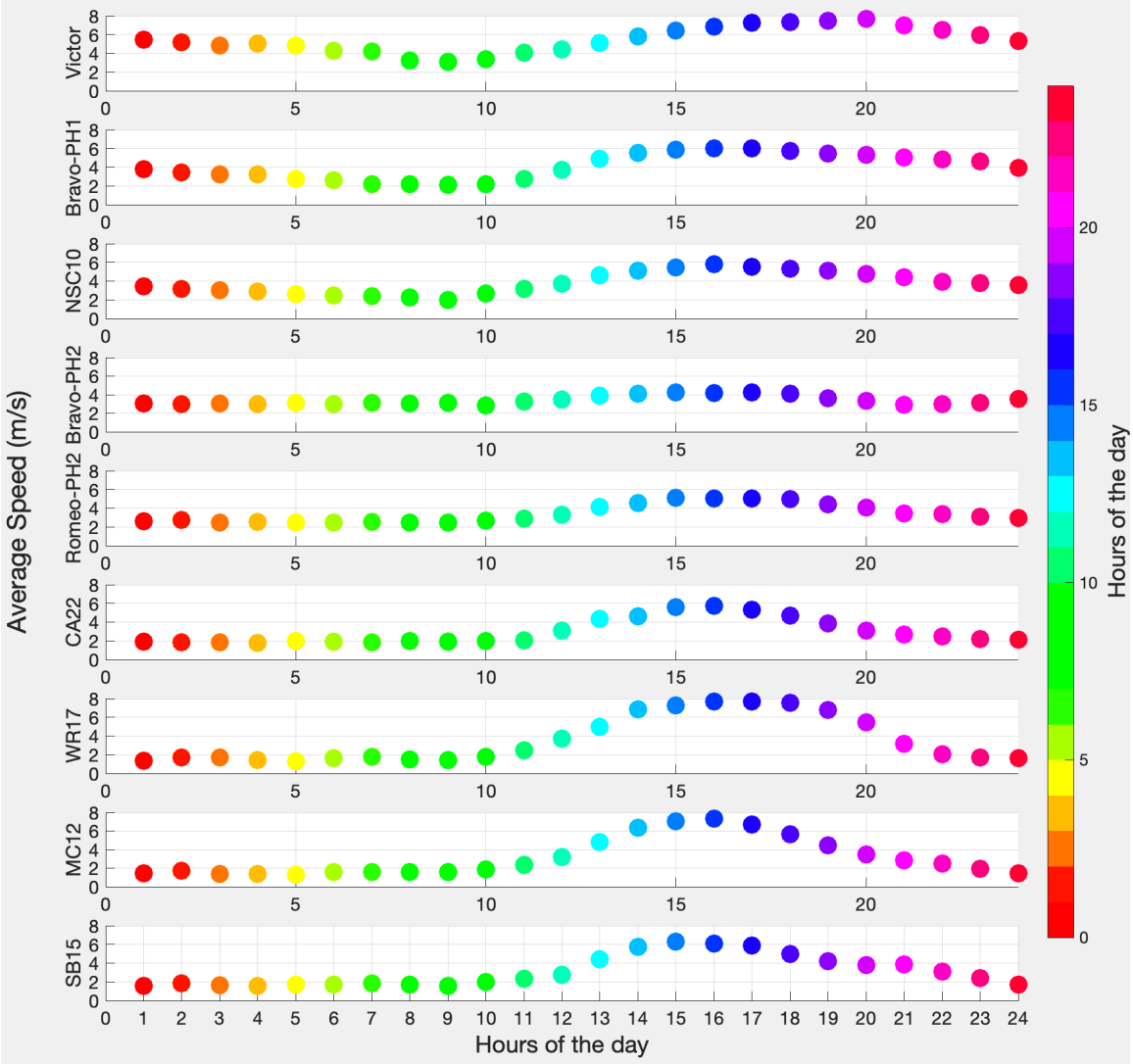

Velocity canonical day for nine selected buoys (three buoys from each phase) displaying the LSB pattern.

Figure 5. LSB Velocity Canonical Day

Coastal wind veering is measured using arrays of buoys (Sand City, Marina, China Rock, Santa Cruz coastline) oriented perpendicular and parallel to the coast. The change in wind angle over distance is plotted for each hour. Wind speeds less than 1.5m/s are filtered out as they were determined too light and variable to represent the wind velocity well.

Differential Kinematic Properties (DKP) of vorticity, divergence, shear, and stretch are computed for triangles of buoys in Phase 2 & 3 using the Bellamy Method (Davies-Jones 1992), which assumes a linear wind field between buoys, where,

$$Vorticity, \zeta = \frac{dv}{dx} - \frac{du}{dy} \quad (1)$$

$$Divergence = \frac{du}{dx} + \frac{dv}{dy} \quad (2)$$

$$Shear = \frac{dv}{dx} + \frac{du}{dy} \quad (3)$$

$$Stretch = \frac{du}{dx} - \frac{dv}{dy} \quad (4)$$

All DKPs were normalized by dividing by the Coriolis parameter (f). Wind speed eastings and northings are averaged using a moving mean by averaging two hours ahead and one hour behind for each hour. DKPs are computed at the center points of each triangle (with corners delineated by buoy location) for each hour. Maximum triangle combinations for each phase are 816 for Phase 2 using 18 buoys and 120 for Phase 3 using 10 buoys.

Triangles are filtered by aspect ratio, timeseries length of the DKP, and whether the imaginary side of a triangle crosses over land (which would violate the linear wind field assumption between sensors). Aspect Ratio, a, is computed as (Ohlman et al. 2017)

$$a = \frac{L_{minor}}{L_{major}} \quad (5)$$

where L_{major} is the maximum distance between the buoys and, L_{minor} is the maximum distance between buoys orthogonal to the L_{major} direction. All triangles with a< 0.24 are filtered out as the triangle shape was determined to not represent an equilateral triangle. DKP timeseries with less than 72 hours of data are filtered out as they were determined to not give an accurate enough representation of DKP at the center point location. Triangles with sides that cross over land are filtered out as the assumption of a linear wind field between buoys does not hold due to topographic interference. A few exceptions to the land crossing filter are included to ensure spatial coverage of DKP triangles around the Monterey Peninsula and the peninsula located west of Santa Cruz Harbor, Steamers Lane.

After filtering, 12 triangles are used from each phase to analyze DKP change, specifically vorticity generation. Due to the natural orthogonal shape of the tip of the Monterey Peninsula, Phase 2 DKPs were rotated 31 degrees counterclockwise to create a local coordinate system in which the positive-y direction is alongshore on the west side of the peninsula, and positive-x direction is alongshore along the north side of the peninsula. Phase 3 DKPs were not rotated as the Santa Cruz coastline is principally east to west.

Manufacturer instrument sensitivity is used in a simple Montecarlo model to determine vorticity error with a comparison to equilateral triangle size. Equilateral triangle size is characterized by the Length Scale (Olhman et al. 2017) calculated by:

$$Length\ scale = \frac{L_{minor} + L_{major}}{2} \tag{6}$$

Figure 6 shows how Vorticity Standard Deviation from manufacture instrument sensitivity changes with triangle Length Scale and wind speed. The Length Scales for the 24 triangles selected in Phase's 2 & 3 are denoted as black lines. Colored lines denote the standard deviation of the vorticity normalized by the Coriolis parameter (f) for different wind speeds. The largest standard deviation are for higher wind speeds with smaller length scales. Instrument induced vorticity standard deviations are less than 0.8 for all triangles used in this paper.

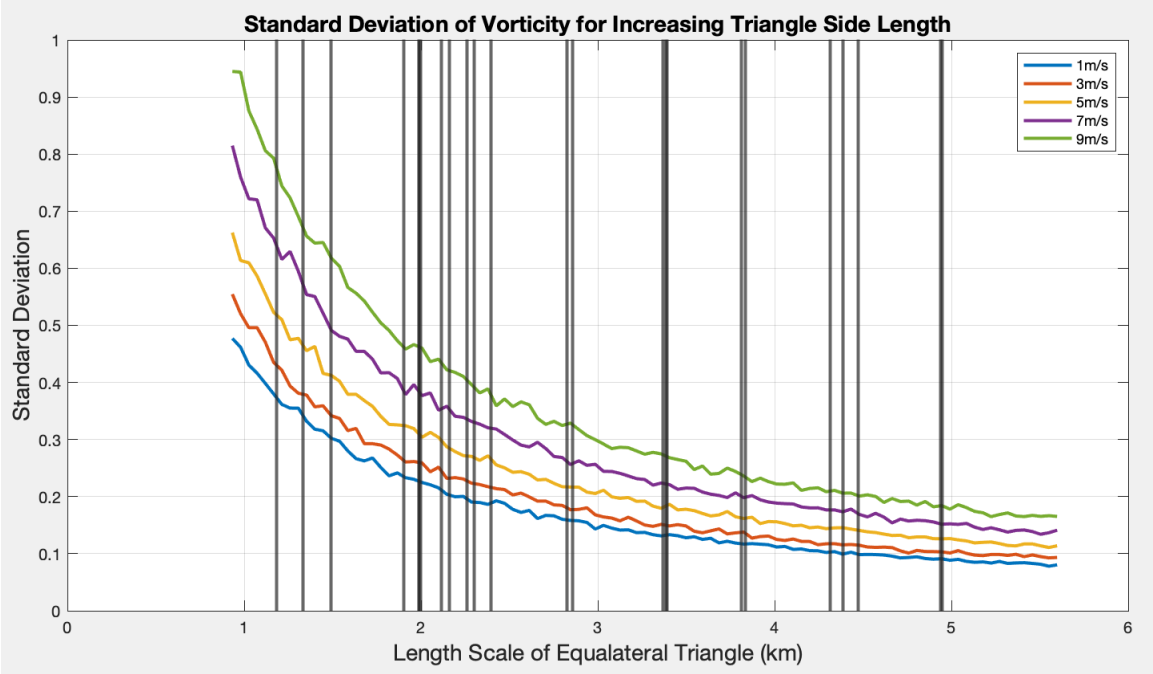

Comparing the Length Scale for an equilateral triangle with vorticity standard deviation for different wind speeds. Black lines are Length Scales of the chosen triangles for Phases 2 & 3.

Figure 6. DKP Error from Instrument Accuracy

Vorticity and shear canonical days are created for each center by averaging the DKP timeseries for each hour of the day to examine the average change in DKP over the day.

The normalized Okubo-Weiss parameter (OWn) is calculated using the DKP to better understand how rotational vorticity compares with shear-induced vorticity. The Okubo-Weiss Parameter is normalized by dividing by the total DKP in the numerator of the equation.

$$OWn = \frac{Stretch^2 + Shear^2 - Vorticity^2}{Stretch^2 + Shear^2 + Vorticity^2} \quad (7)$$

If OWn is between 0 and 1, shear and stretch DKP dominate the rotational vorticity. If OW is between -1 and 0, rotational vorticity dominates the shear and stretch.

THIS PAGE INTENTIONALLY LEFT BLANK

III. RESULTS

A. MONTEREY BAY

Synoptic wind flows into Monterey Bay from the northwest. Wind velocity canonical day for all buoys for all phases is plotted in Figure 7. Wind hugging the Santa Cruz coastline (most northern buoys) experiences dramatic shifts in wind direction over the day as the LSB takes effect, as well as due to shear from the coastline. Winds in the middle of the bay are largely onshore with a northern shift in wind direction seen throughout the day intensifying with decreasing distance to shore. This northern shift in onshore wind direction is also apparent at Marina and Sand City.

As synoptic winds encounter Monterey Peninsula, a shift in winds is noticed depending on the time of the day and the strength of the LSB. Winds on the northern half west side of the peninsula tend to flow north and clockwise around the peninsula at all times of the day and increase in speed when the LSB is at its maximum. During the afternoon and evening when LSB forcing is strongest, winds on the southern half of the west side of the peninsula flow northeast around the peninsula and into the bay. During the night and early morning, winds on the southern half of the west side of the peninsula tend to shift to the synoptic flow out of the northwest and flow south of the peninsula.

The strongest relative magnitude winds are seen during the afternoon and evening at all buoys. Spatially, the strongest winds occur far from shore over the open ocean, along the Santa Cruz Coastline, and within southern Monterey Bay near Marina and Sand City.

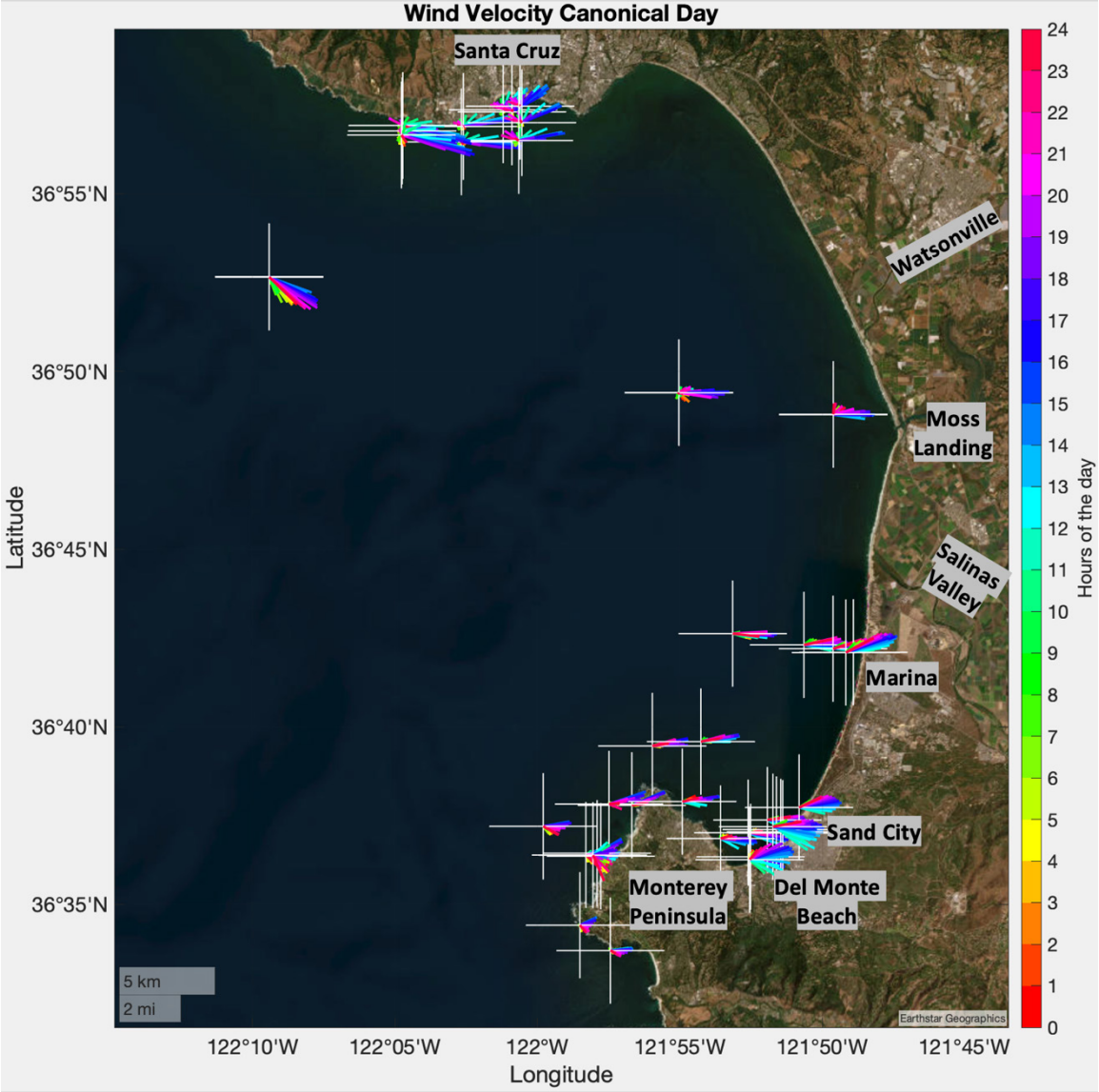

Wind velocity canonical day for all buoys in all phases.

Figure 7. All Phase Wind Velocity Canonical Day

B. PHASE 1

Coastal wind backing and veering during Phase 1 are analyzed at Sand City and Marina. Wind velocity canonical day is calculated for all buoys in each phase, with all times being local (UTC -8). Wind barbs show the direction the wind is flowing and are measured in degrees clockwise from North (i.e., East = 90 degrees, West = 270 degrees). The magnitudes of the vectors are relative. Average offshore winds located at buoy Victor

(Figure 8, Left) are out of the northwest and vary between 119 and 168 degrees throughout the day, corroborating the synoptic flow seen in previous studies (Darby and Banta 2002). Victor average maximum wind magnitudes occur in the afternoon and evening, with the most westerly winds seen between 1200–1700L and most northerly winds seen between 0300–1000L with smaller average magnitudes.

The Sand City buoy array length is slightly over 1km long. The wind velocity canonical day for the Sand City buoy array (Figure 8, Right) shows the most northerly winds occurring in the late morning between 1000–1200L. As the land heats up, pressure differential builds, and the LSB starts. The winds at all buoys begin to back with time, becoming more westerly and increasing in magnitude. By late afternoon the winds have reached peak magnitude, and the land starts to cool, decreasing the intensity of the pressure gradient associated with the LSB. From midnight to 1000L, winds from the LSB reach their peak backing angle. Minimum wind speed magnitudes are reached between 0400 and 0900L, substantiating observations of a pressure gradient at night between Monterey and Santa Cruz seen in Archer & Jacobson (2005). Winds then shift to their most northerly angle, perpendicular to the shore, once the LSB begins in the late morning. The backing of winds over time due to the LSB is significant but also expected. Also noticeable is the backing of winds at the same hour as the distance from the furthest buoy to the coastline decreases.

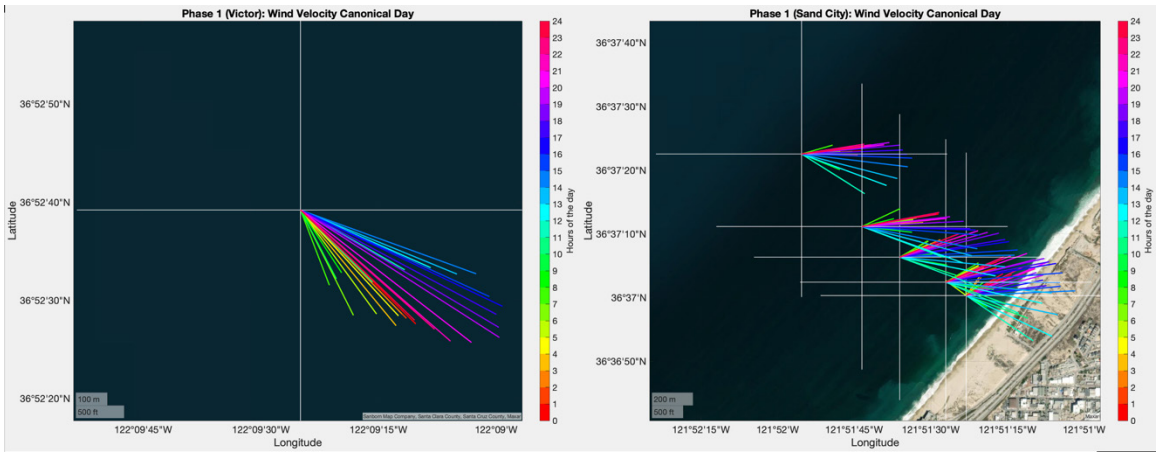

(Left) Canonical day for Victor located farthest offshore in the middle of the bay. (Right) Canonical day for buoy array at Sand City, CA. Buoys include: Whiskey, SC20, SC15, SC10, SC07 (offshore to onshore).

Figure 8. Phase 1 Wind Velocity Canonical Day

The magnitudes of the average wind speed at the farthest offshore buoy from the Sand City array, Whiskey shows a recognizable LSB pattern (Figure 9, Top). Average wind speed maximums reach 5.75m/s at 1600L, and average wind speed minimums reach 2.4m/s at 0800L. The change in wind direction at each hour at buoys from offshore towards the shore are compared to hourly winds at Whiskey (Figure 9, bottom). Negative Delta Theta means a decrease in wind angle (a counterclockwise shift, or backing of winds with distance to shore) for that buoy at that hour when compared to Whiskey, while a positive Delta Theta indicates a veering of winds with decreasing distance to shore. A backing of winds is apparent at all times except during the early morning from 1000 to 1300L when Delta Theta is positive. This positive Delta Theta veers the winds as the LSB restarts and redirects the winds to be more northerly and perpendicular to the shore.

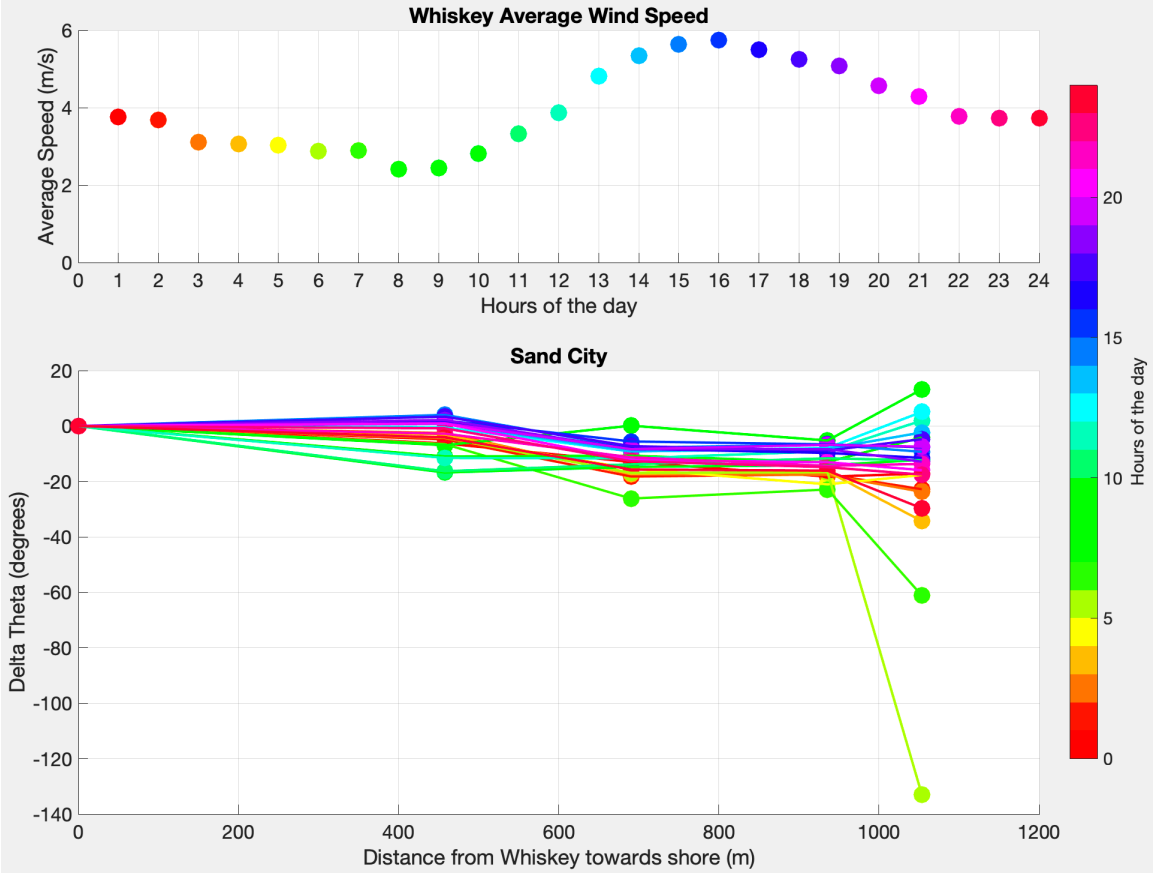

(Top) Canonical day average wind speed for buoy Whiskey (array buoy farthest offshore). (Bottom) The change in angle from wind direction at Whiskey with decreasing distance to shore at each hour.

Figure 9. Phase 1 Sand City Coastal Wind Backing

The wind velocity canonical day for the Marina buoy array is almost 6.5 km long (Figure 10). The LSB pattern of wind speed and direction is similar to the pattern seen at Sand City, with most northerly winds seen in the late morning and most southerly winds seen in the early morning before the initiation of the LSB. Winds at the buoy farthest from shore (Bravo) are largely westerly with minimal changes in angle throughout the day, while winds at buoys closer to shore have larger wind angle ranges. Due to the increased length of the array, the backing with distance to shore is more apparent than at Sand City.

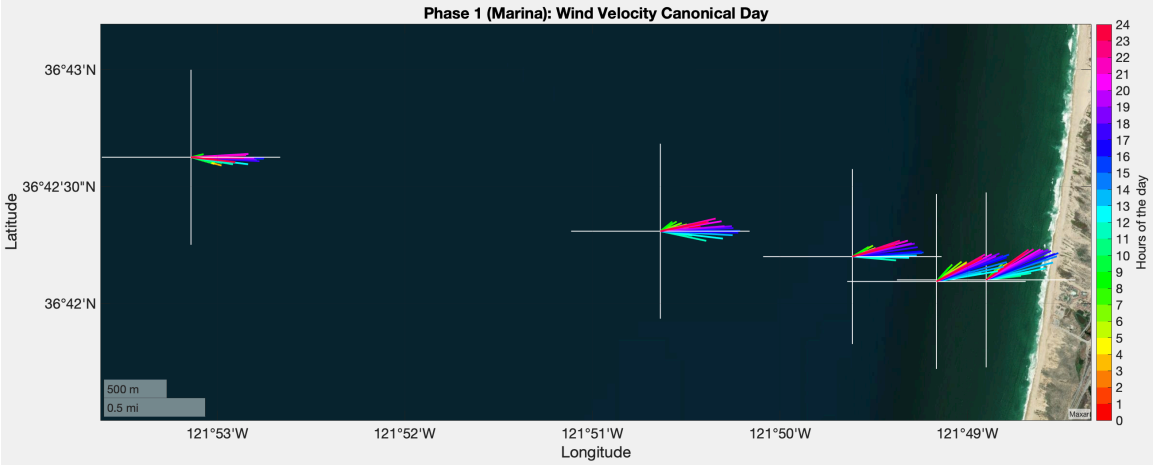

Buoys include: Bravo, Gulf, Romeo, MAR18, MAR12 (offshore to onshore).

Figure 10. Marina Array: Wind Velocity Canonical Day

Bravo average wind speed (Figure 11, Top) follows the same LSB trend seen at buoy Whiskey at Sand City. Maximum and minimum average winds occur an hour later than Sand City at 1700L and 0900L with magnitudes 6.04m/s and 2.58m/s, respectively. This is most likely due to Bravo's increased distance from shore compared to Whiskey. Bravo average wind speed maximums and minimums are also slightly higher (~0.2m/s) than those seen at Whiskey.

Wind backing with distance to shore is apparent from the negative Delta Theta seen at almost every hour at Marina (Figure 11, Bottom). Moving shoreward, Delta Theta continues to become steadily more negative. This means that the difference in wind direction from Bravo (buoy farthest offshore) continues to decrease, with winds becoming more southerly as distance to shore decreases. At the beginning of the LSB (1200-1300L), the wind backing is the least noticeable, with Delta Theta around -20 degrees from Bravo to MAR12 (the buoy closest to shore). As the day progresses, the backing continues to increase in magnitude, even as the wind speed magnitude from the LSB declines at night and early morning. The largest Delta Theta occurs between -45 to -55 degrees (most southerly winds) in the early morning between 0400–0900L when winds are the lightest. Around 1000L the LSB begins to set up, and the system resets itself.

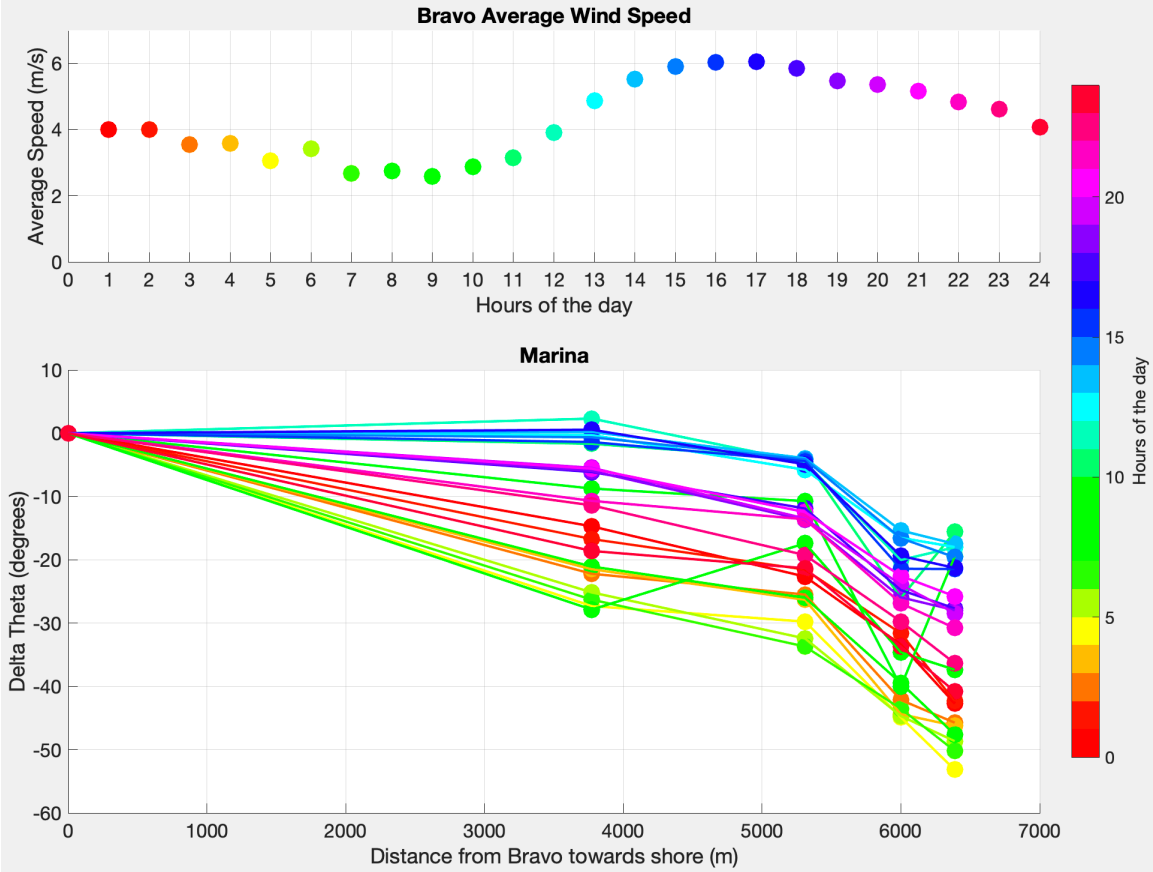

(Top) Canonical day average wind speed for buoy Bravo (array buoy farthest offshore). (Bottom) The change in angle from wind direction at Bravo with decreasing distance to shore at each hour.

Figure 11. Phase 1 Marina Coastal Wind Backing

Wind speed, easting, and northing are shown with decreasing distance to shore at Marina (Figure 12). The diurnal cycle of the LSB is apparent, with max wind speeds between 1500–1700L and minimum wind speeds between 0700–1000L at all buoys in the array (Figure 12, Top). Wind eastings (Figure 12, Middle) also follow this same trend. Additionally, as winds flow towards the shore, the wind speed, along with wind speed easting stay relatively constant. Wind northings have maximums at different times depending on how close the buoy is to shore (Figure 12, Bottom). Buoys farther offshore have maximum northings at night around 2000–1000L, while buoys close to shore have maximum northings in the afternoon to early evening (1700-2200L). Wind northings increase as distance to land decreases.

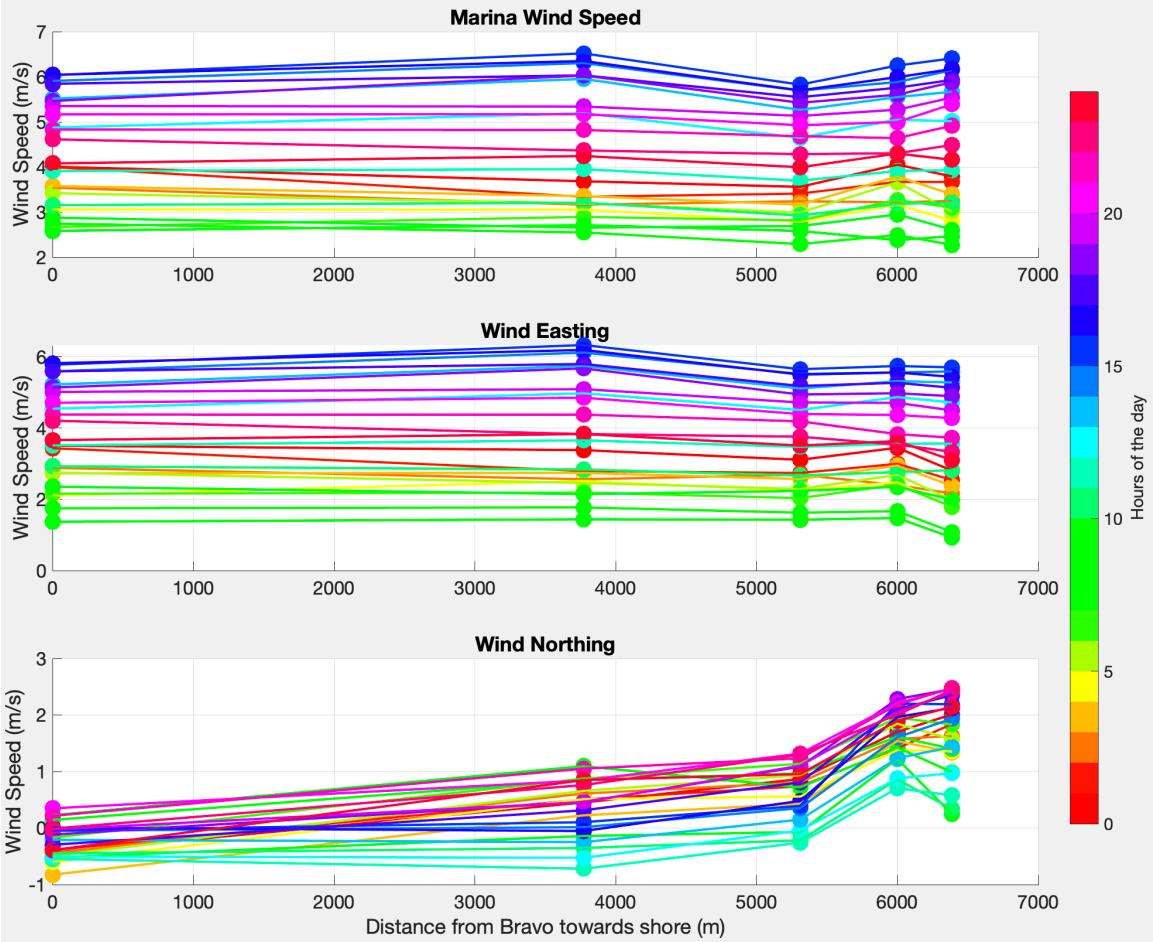

Average Wind Speed (Top), Wind Eastings (Middle), and Wind Northings (Bottom) with decreasing distance to shore.

Figure 12. Phase 1 Marina Wind Speeds

C. PHASE 2

The wind velocity canonical day for buoys surrounding the Monterey Peninsula can be seen in Figure 13 (Left). Buoys to the northern side of the peninsula show the winds predominantly flow northeast around the peninsula and onto Del Monte beach (the eastern-most part of the peninsula where the land begins to curve north).

Winds at China Rock (Figure 13, Right) are more variable in direction than buoys AS40 and AS15 (located just north of the China Rock array) and show a different pattern than what is seen at Sand City and Marina. The most northerly winds are observed at night and in the early morning (2300-1000L) when the influence of the LSB is at a minimum

and the synoptic flow pattern from the northeast is dominant. The influence of the LSB can be seen in the afternoon and evening (1400-2000) as the winds become the most southerly of the day with the largest magnitude. The array shows the spreading of the wind vector directions with decreasing distance to shore as the flow becomes disrupted by the presence of land.

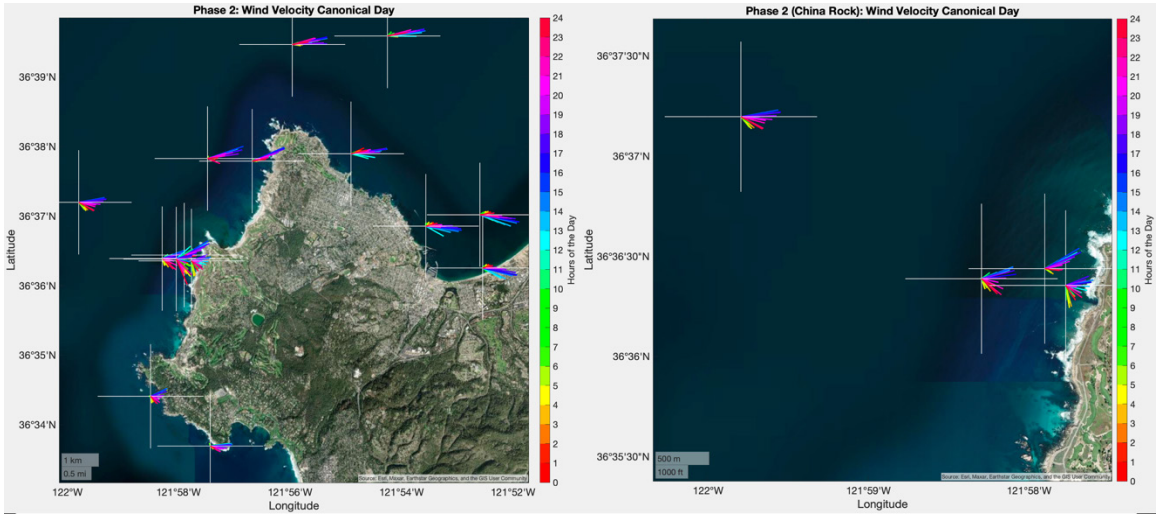

(Left) Canonical day for buoys surrounding Monterey Peninsula. (Right) Canonical day for buoy array at China Rock. Buoys include: Bravo, CR30, CR16, and CR10 (offshore to onshore).

Figure 13. Phase 2 Wind Velocity Canonical Day

Bravo average wind speeds show a maximum of 4.3 m/s between 1500–1700L and a minimum of 3.1 m/s between 2100–1000L (Figure 14, Top). Though less apparent than the buoys within Monterey Bay, the effect of the LSB on wind speed is noticeable with the increased wind speed between the hours of 1100–2000L.

During the hours that the LSB winds influence the buoys (1100-2000), Delta Theta is negative (up to -20 degrees), meaning the winds have backed to be out of the south, driving the winds towards Monterey Bay as the winds flow northeast around the peninsula (Figure 14, Bottom). The winds outside of the LSB timeframe show a positive Delta Theta (up to 40 degrees), meaning the winds veer and become more northerly as distance to shore decreases.

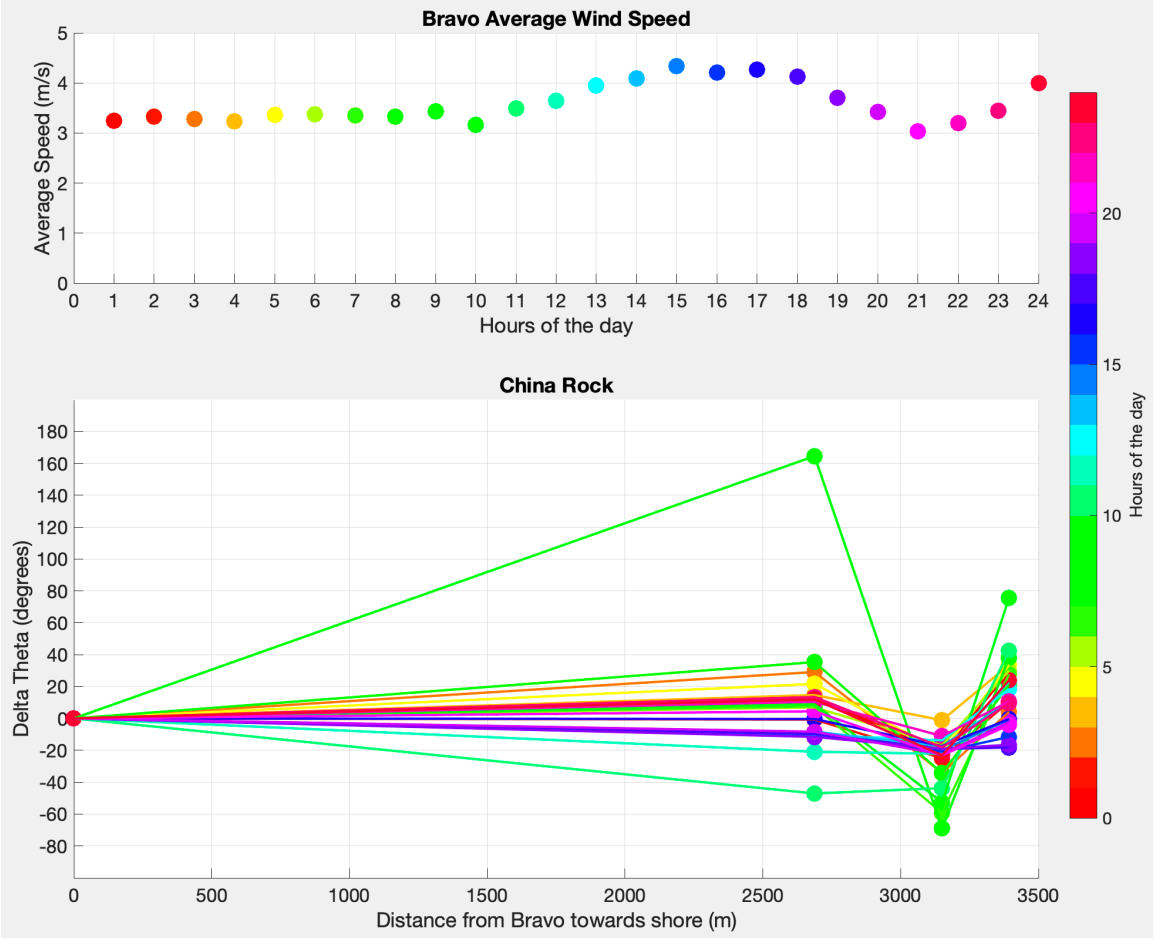

(Top) Canonical day average wind speed for buoy Bravo (array buoy farthest offshore). (Bottom) The change in angle from wind direction at Bravo with decreasing distance to shore at each hour. Buoy CR20 was left out due to the buoy being deployed for only three days, potentially leading to biased results if incorporated.

Figure 14. Phase 2 China Rock Coastal Wind Veering and Backing

Average alongshore vorticity is plotted at center points between buoys transiting around Monterey Peninsula (Figure 15, Left). Center A is slightly negative (a value of -0.61), which lines up well with how the wind flow directions near this point change direction during the LSB influence seen in Figure 14. Average positive vorticity at Centers B & C (0.15 and 1.32, respectively) reflect the average winds turning counterclockwise due to the flow inhibition caused by the peninsula. Centers D through L shows negative vorticity values caused by the wind turning clockwise, following the coastline around the peninsula, and encountering drag from friction. Maximum average vorticity is seen at centers D & L with values of -3.29 and -4.5.

The average alongshore Normalized Okubo Weiss parameter is plotted in Figure 15 (Right) and shows all positive numbers at each of the center points. This means that the majority of the vorticity created around the peninsula is shear or stretch-induced instead of being created by rotational vorticity. Higher positive values (between 0.64 and 0.79) of the Normalized Okubo Weiss parameter can be seen in the center points to the west of the peninsula (A-C), while the center points to the east (D-L) have smaller magnitude positive values close to 0.3.

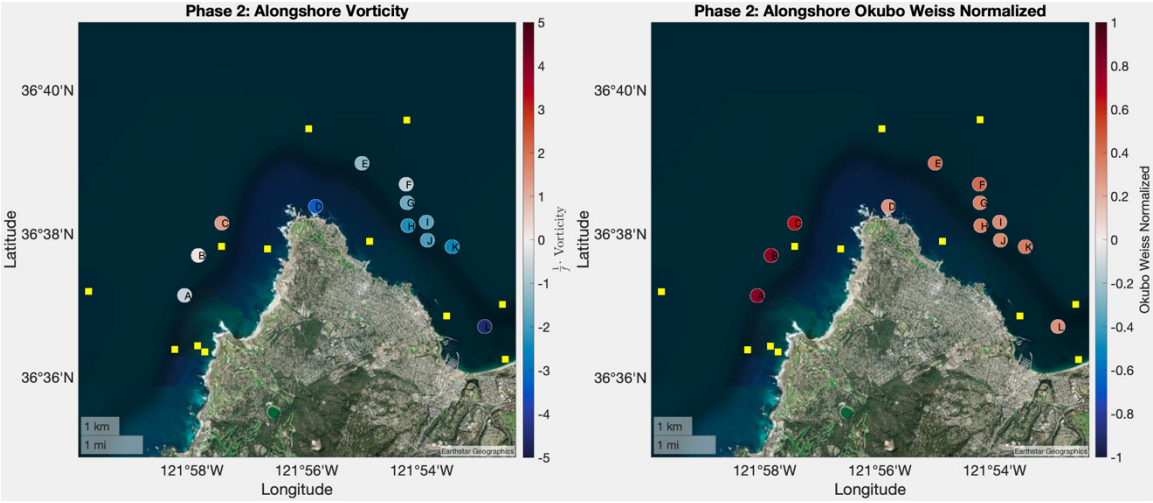

(Left) Average vorticity for 12 center points surrounding Monterey Peninsula. (Right) Average normalized Okubo Weiss parameter for 12 center points surrounding Monterey Peninsula.

Figure 15. Phase 2 Average Alongshore Vorticity and Normalized Okubo Weiss

Alongshore vorticity canonical days are plotted for each center point and show how vorticity at that location changes throughout an average day. Notably, almost all center points show an increase in vorticity magnitude during the afternoon and evening (1000-2000L), coinciding with the LSB timeframe, and near zero values in the morning before the LSB begins. Center C shows the positive vorticity seen west of the peninsula in Figure 14 (Left), maximizing around 3 times the Coriolis parameter at 1400L. Large negative vorticity values can be seen at Centers: D-L, with maximum vorticity values around 8 times greater than the Coriolis Parameter at Center L between 1500–2100L.

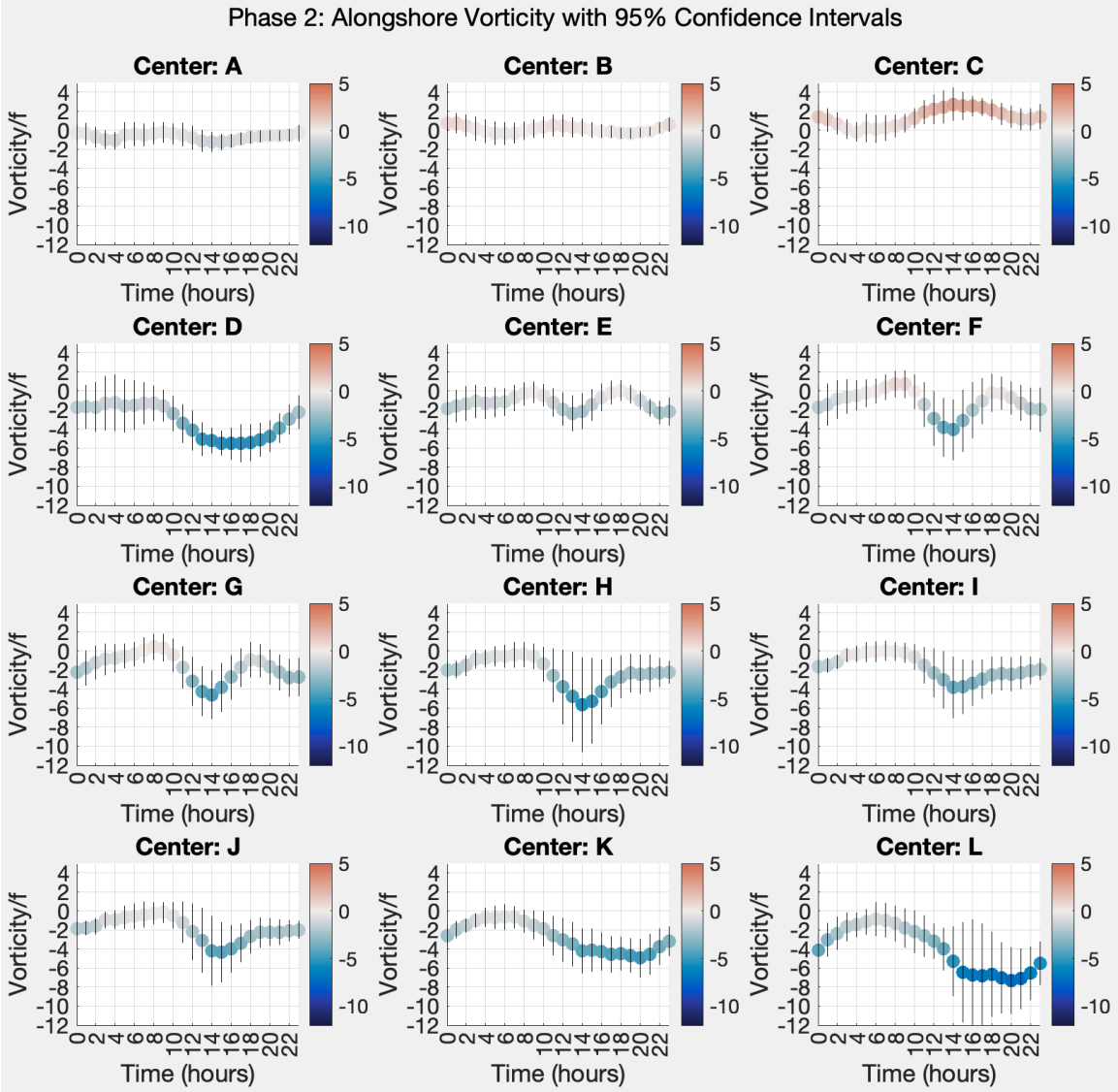

Alongshore Vorticity Canonical Day with 95% Confidence Intervals for the 12 center points.

Figure 16. Phase 2 Alongshore Vorticity Canonical Day

Alongshore shear canonical days are plotted for each center point and show how shear at that location changes throughout an average day (Figure 17). Shear at centers A-C all show a positive increase in shear (creating clockwise rotation) during the afternoon when the LSB is at its peak. Centers D-L show a varying degree of positive and negative shear over the canonical day with larger confidence intervals, meaning there is a large degree of change and uncertainty throughout the day associated with alongshore shear on

the northeast side of the peninsula. Centers H, I, and J all show a peak in negative shear during the afternoon.

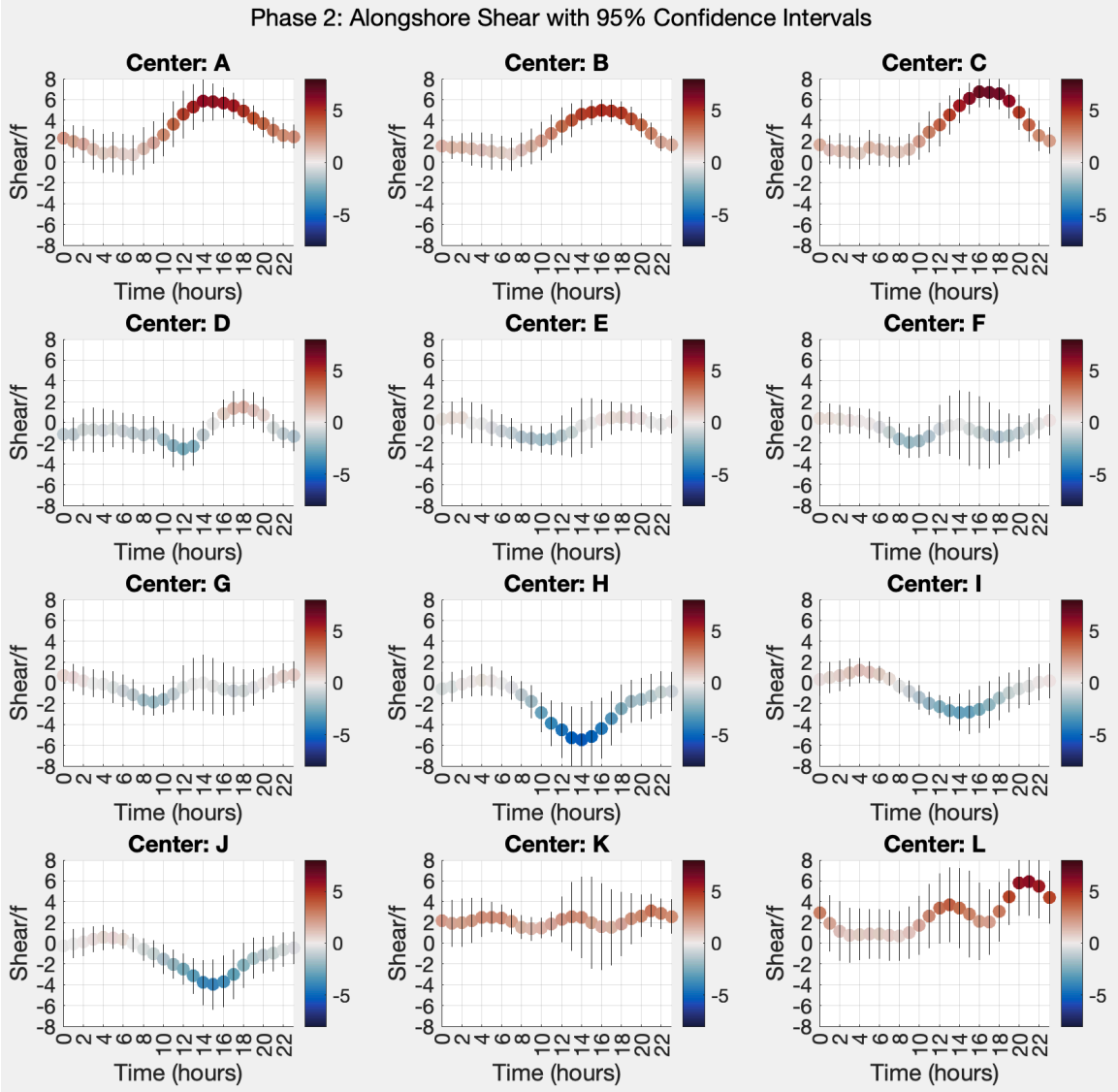

Alongshore Shear Canonical Day with 95% Confidence Intervals for the 12 center points.

Figure 17. Phase 2 Alongshore Shear Canonical Day

D. PHASE 3

Wind velocity canonical day is plotted for the Santa Cruz buoys and shows the daily changes in wind speed and direction due to the LSB (Figure 18). The strongest wind speeds

are westerly and occur during the afternoon and evening (1300-2000L) at all buoy locations. Once the LSB begins to die down, the winds become southeasterly and flow onshore with decreased magnitudes. Alongshore backing of winds can be seen in the east around Steamers Lane compared to the winds at buoys farthest west.

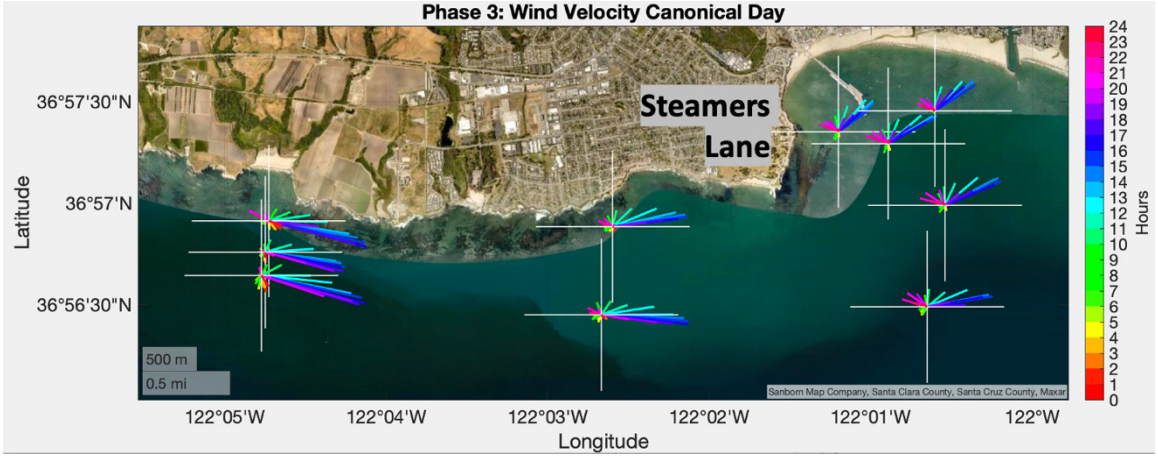

Wind Velocity Canonical Day for all ISPAR buoys used in Phase 3.

Figure 18. Phase 3 Wind Velocity Canonical Day

The average canonical wind velocity for buoy WR17 is plotted in Figure 19 (Top) and displays a LSB pattern. Average wind maximums reach just under 8m/s in the afternoon (1500-1900L), while average wind minimums reach around 2m/s during the night and early morning (0000-1000L). The Delta Theta of the alongshore winds (Figure 19, Bottom) shows backing (negative Delta Theta) at almost all hours of the day except in the early morning, where winds are light, and backing is negligible. Maximum backing is seen between the hours of 1900–0000L with Delta Theta angles between 90 and 170 degrees. Backing angles during the maximum wind speeds, when the LSB is at its greatest influence, are between 40 to 60 degrees.

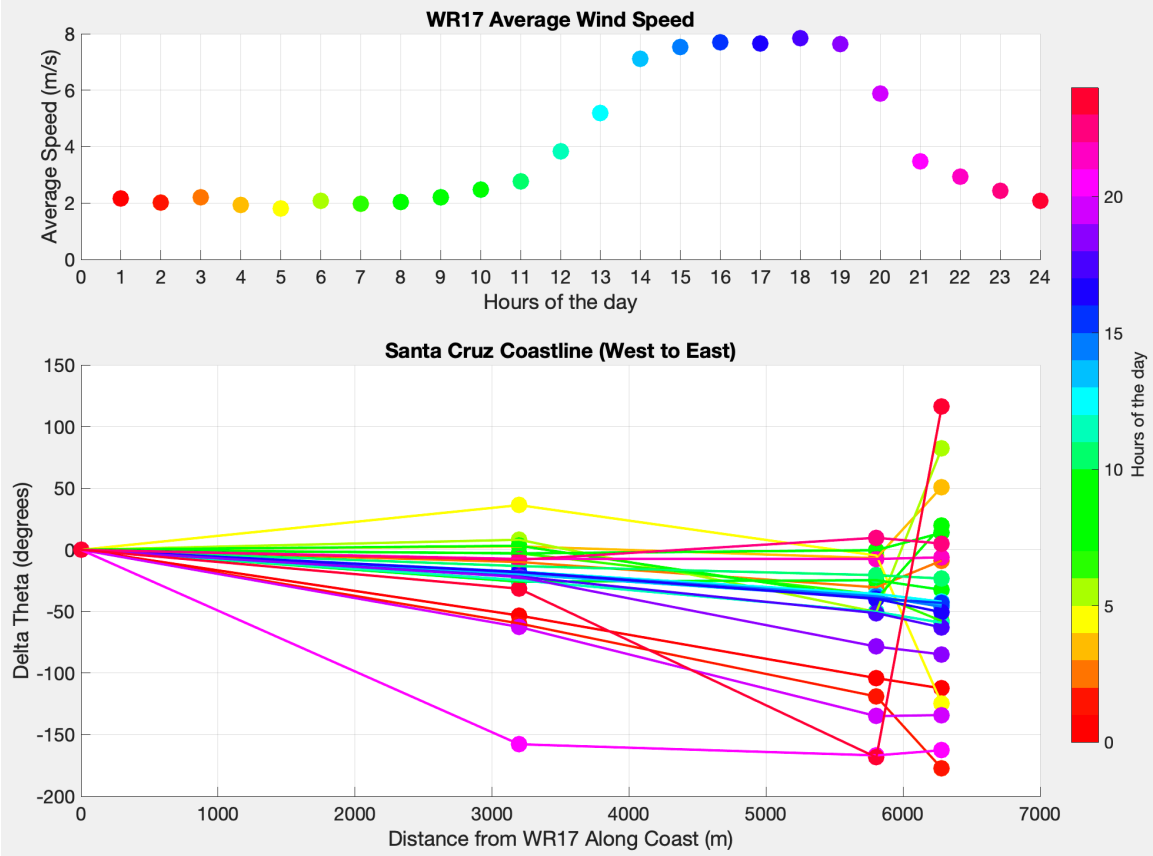

(Top) Average wind speed magnitude at buoy WR17 (buoy located farthest west). (Bottom) The change in angle from wind direction at WR17 with increasing distance alongshore at each hour. Buoys include: WR17, MC12, P12, and SB10.

Figure 19. Phase 3 Santa Cruz Alongshore Backing

Vorticity is plotted for 12 center points along the Santa Cruz coast (Figure 20, Top). Average vorticity around Santa Cruz is positive at all center points, likely due to friction from the coastline, confirming model results seen in Tseng et al. (2011). Average vorticity at centers A & B is around 10 times the Coriolis parameter, while average vorticity maximums are observed near Steamers Lane with magnitudes between 4.9 (Center H) and 15 (Center G). Average vorticity decreases in magnitude within the harbor to become around 3.4 at Center K and 2.2 at Center L.

Like Phase 2, the average normalized Okubo Weiss parameter (Figure 20, Bottom) displays only positive values, meaning the DKP of shear and stretch dominate rotational vorticity in the area. Maximum OWn values are seen at Centers A, B, H, & L between 0.46

and 0.49. Minimum OWn values can be seen where vorticity is large (Centers G, C, & J) and range from 0.13 to 0.23.

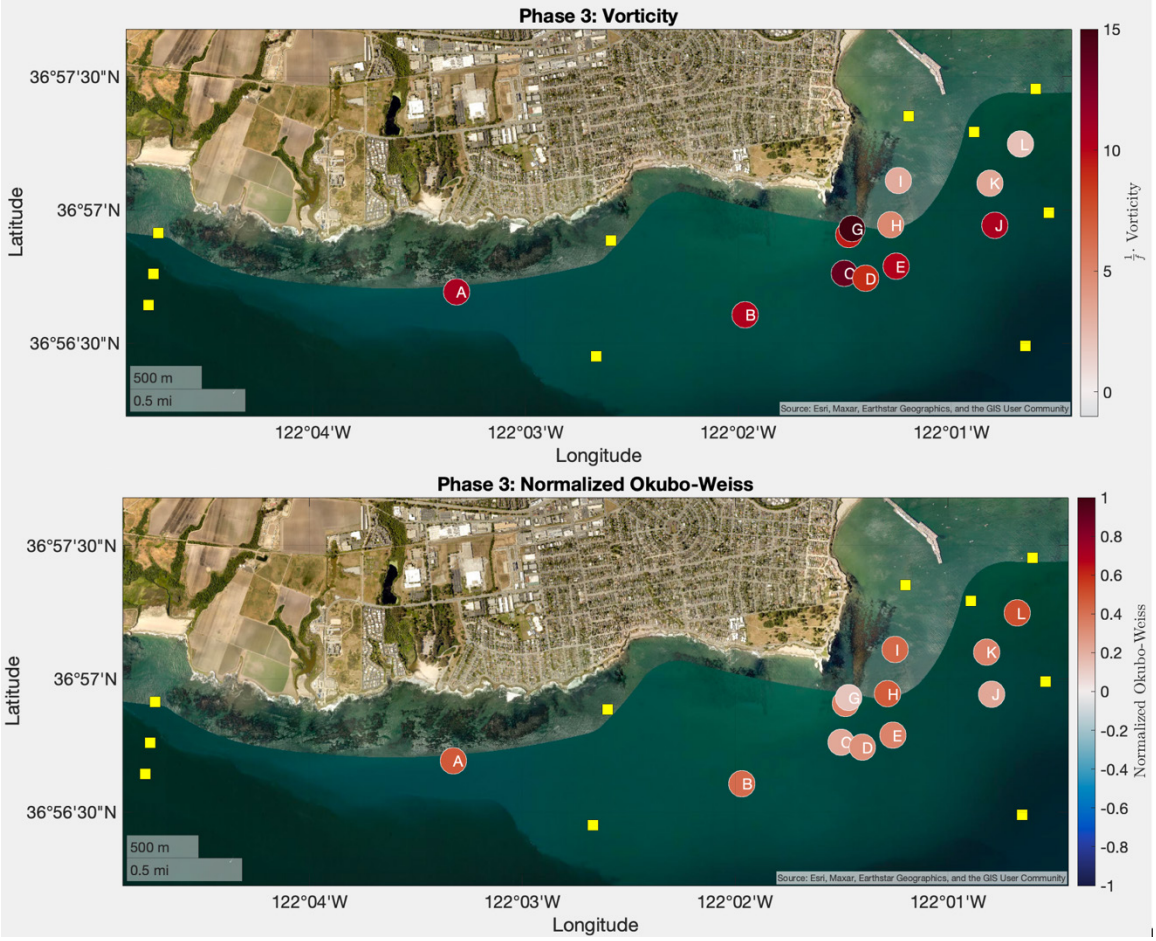

(Top) Average vorticity for 12 center points off Santa Cruz. (Bottom) Average normalized Okubo Weiss parameter for 12 center points off Santa Cruz.

Figure 20. Phase 3 Average Vorticity and Normalized Okubo-Weiss Parameter

Vorticity canonical days are shown for all center points in Phase 3 with a noticeable LSB diurnal pattern (Figure 21). Positive vorticity maximums are seen at all centers between 1600–1900L. Maximum vorticity values are seen at Center G, located closest to Steamers Lane, and are between 40 to 50 times greater than the Coriolis parameter. Minimum vorticity values at all centers are observed in the early morning between 0600–1100 and range between -5 and 5.

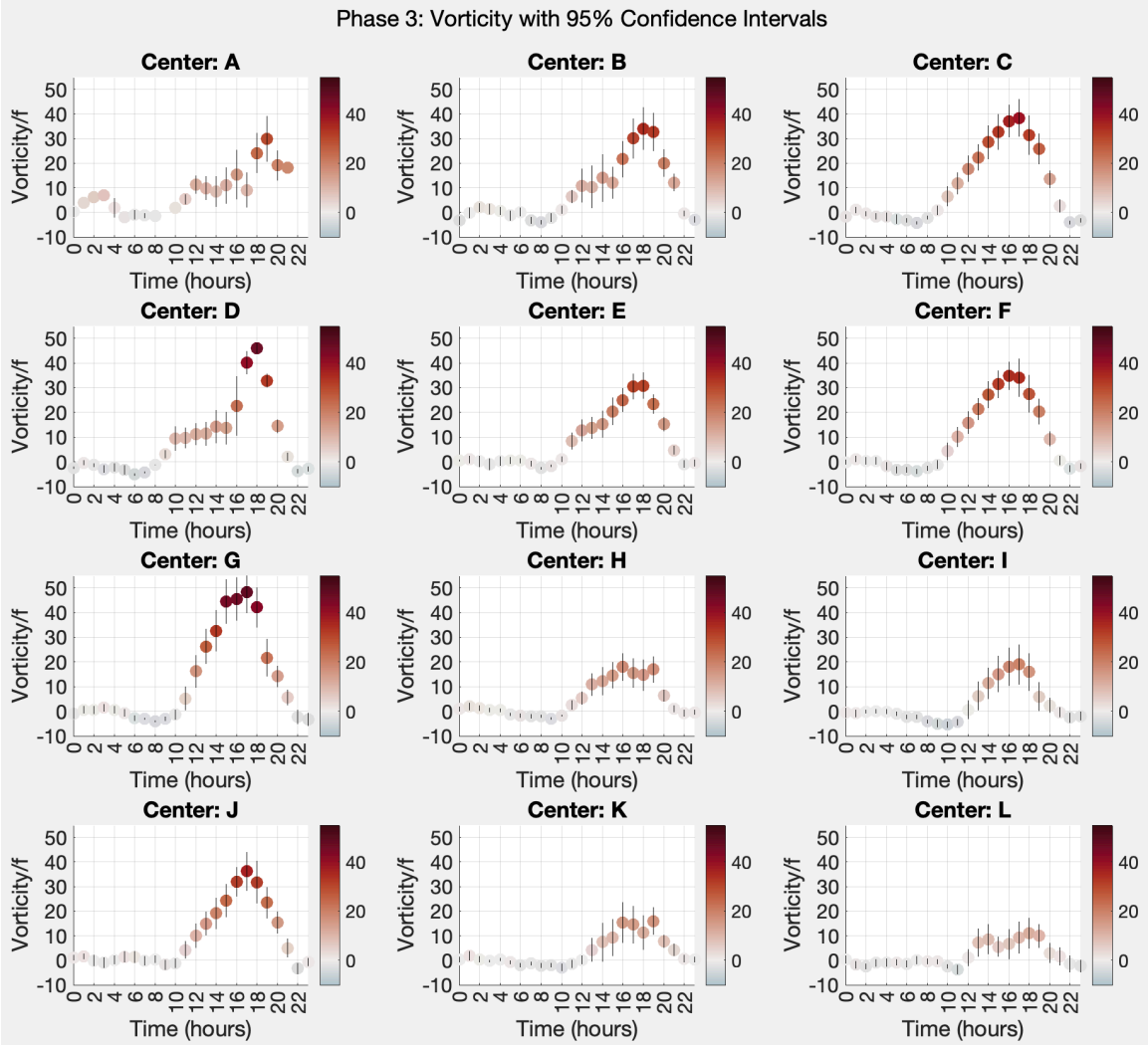

Vorticity Canonical Day with 95% Confidence Intervals for the 12 center points.

Figure 21. Phase 3 Vorticity Canonical Day

The average shear canonical day shows a peak in negative shear (counterclockwise rotation) during the peak hours of the LSB (Figure 22). Largest values of shear are seen around Steamers Lane with values between -25 to -35. During hours where the LSB is relaxed, shear at all locations is slightly positive, ranging between 0 to 8.

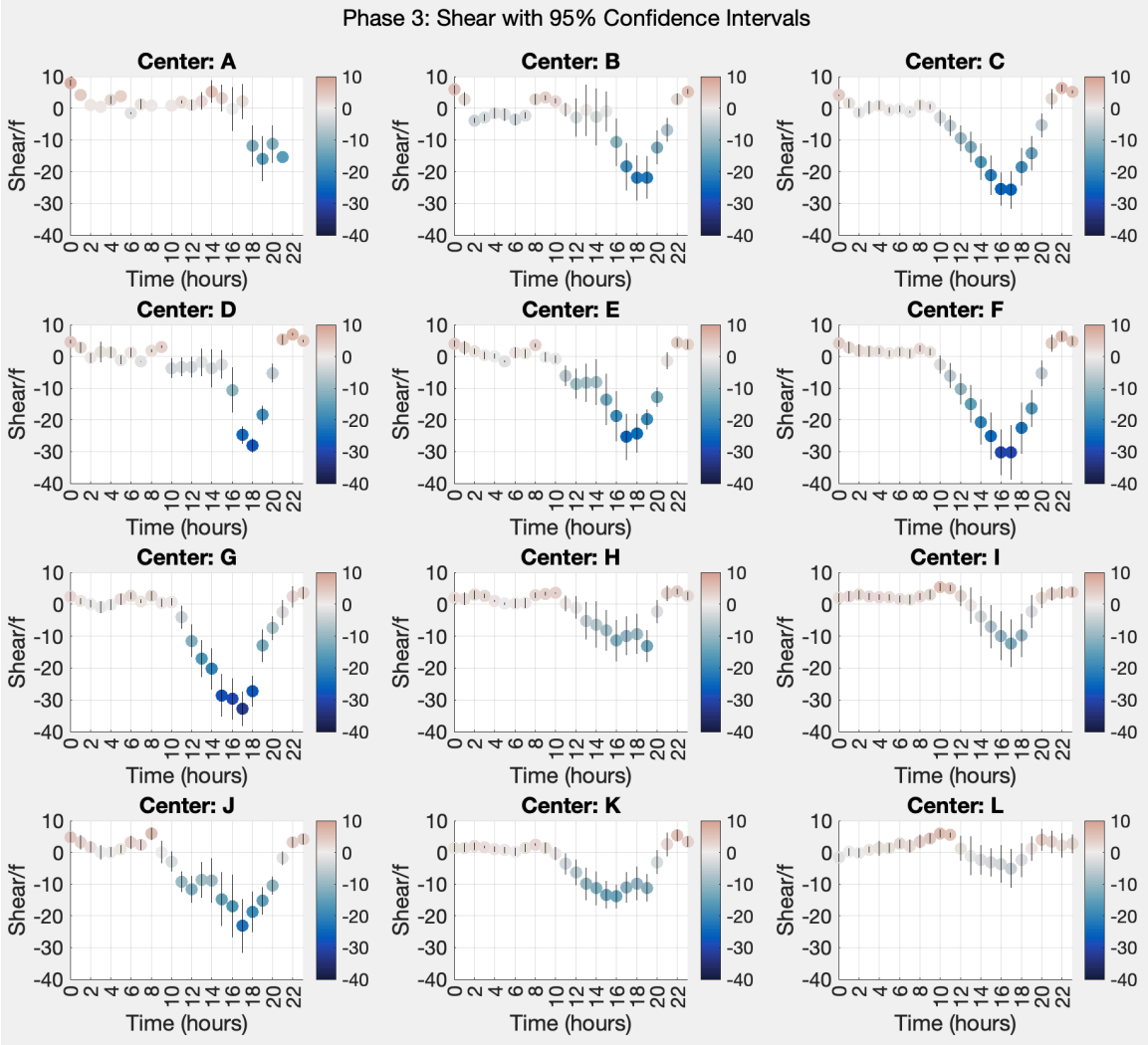

Shear Canonical Day with 95% Confidence Intervals for the 12 center points.

Figure 22. Phase 3 Shear Canonical Day

IV. DISCUSSION

The two types of wind veering and backing observed within Monterey Bay are temporal and spatial. Temporal veering and backing is the change in wind direction at one location over time. Spatial veering is the change in wind direction alongshore or with decreasing distance to shore. Additionally, the response to spatial wind veering and backing that induce cross-shore and alongshore spatial gradients in the wind, can be described with DKPs.

A. TEMPORAL VEERING AND BACKING

The nighttime pressure gradient forcing winds to flow from Monterey to Santa Cruz, documented by Archer and Jacobson (2005), helps explain the temporal backing seen at all buoys within Monterey Bay. Winds along the Santa Cruz coastline show a distinct temporal change in direction, with westerly winds seen during the peak LSB hours due to the increased heating and pressure differential set up over central Monterey Bay (Salinas Valley and Watsonville) and southerly onshore winds seen at night. Temporal backing of surface winds in southern Monterey Bay throughout the canonical day also supports a north-south pressure gradient. Winds on the west side of Monterey Peninsula are also affected by the LSB pressure gradient during the day, although winds on the southern half of Monterey Peninsula less influenced by the nighttime north-south pressure gradient as winds are observed to become northwesterly and flow in the direction of the synoptic winds.

B. SPATIAL VEERING AND BACKING

Wind spatial backing was measured at Sand City and Marina. Previous cross-shore LSB measurements using a Doppler-lidar within Monterey Bay indicated “onshore flow was most likely to be perpendicular to the shore at the lowest levels” (Darby and Banta 2002). Additionally, previous research suggests offshore wind direction and speed is expected to be similar to winds seen at the sea-land interface, and only change direction once friction increases over land (Roeloffzen et al. 1985). This decrease in speed would decrease the forcing from Coriolis and increasing the influence of the pressure gradient

force, backing the winds (Roeloffzen et al. 1985). The measurements here find, while winds are indeed onshore, the offshore winds at Marina and Sand City change direction before changing wind speed, and likely cross the shoreline at non-perpendicular angles depending on the time of day and strength of the LSB. Wind speeds at Marina (Figure 12, Top) remain relatively constant as distance to shore decreases. Marina wind speed northings increase with decreasing distance to shore, likely indicating a stronger pressure gradient north of Marina at all hours of the day.

China Rock spatial backing and veering is also apparent (Figure 14). Frictional effects of the coastline are observed by the flaring of the canonical day wind vectors with decreasing distance to shore as winds are more forced to flow north or south when encountering the coast. Canonical day winds at CR16 more resemble winds seen at AS40 and AS15 with flow primarily directed north around the peninsula, while CR30 and CR10 canonical day winds flare both north and south, indicating a likely location for a point of wind flow divergence around the peninsula.

Santa Cruz coastline alongshore spatial backing can be seen with the counterclockwise bending of the wind flow near Steamers Lane and into Santa Cruz harbor (Figure 19). Surface winds largely follow the predominantly cliff-like coastline and then encounter the more open area of Santa Cruz Harbor east of Steamers Lane and can spread northward. The topography of the city of Santa Cruz is largely flat; meaning winds can flow onto land without much resistance until the Santa Cruz mountains are encountered 3–4 km inland.

C. DKPs

Phase 2 alongshore DKPs around the northside of the Monterey Peninsula detail the influence of coastal topography and the LSB forcing on the bending of winds around the peninsula (Figure 15). Average vorticity at center A is slightly negative, indicating a clockwise rotation of the average winds, while average vorticity at center C is slightly positive, indicating a counterclockwise rotation of the average winds. In-between centers A and C is center B, whose average vorticity is nearly 0, indicating this region is part of the area where winds shift between turning counterclockwise (north) or clockwise (south).

Average negative vorticity at centers D-L flowing around Monterey Peninsula shows how the wind bends to follow the coastline and encounters friction from the coast to create rotation. The positive normalized Okubo Weiss parameters also indicate the importance of shear and stretch in the coastal wind flow, with shear and stretch having more of an influence on wind flow than vorticity when vorticity is small, as seen on the peninsula's west side.

Phase 2 canonical day alongshore DKPs highlight the large influence of the LSB on the wind flow (Figures 16 and 17). Canonical day vorticity indicates larger negative vorticity values at centers D-L during peak LSB hours in the afternoon. It is worth noting that large confidence intervals are seen at many hours at these centers, meaning winds are highly variable, although the 95% confidence intervals are still less than 0. Vorticity at centers A & B are all close to 0 at all hours of the day, indicating that while the LSB does influence the winds at those buoys, rotation is largely negligible. Positive vorticity at center C during the peak LSB timeframe indicates the counterclockwise shifting of winds during this time. Canonical day alongshore shear values indicate a more complicated wind flow dynamic. Alongshore shear at centers A-C all show an increase in positive shear values (creating clockwise rotation) due to the LSB in the afternoon. Centers D-G have largely variable canonical day alongshore shear values, most likely due to the wind flowing east away from the coast, meaning the eastern peninsula coastline initially plays a small influence on wind flow dynamics. As winds turn and become more alongshore to the eastern side of the peninsula, centers H, I, and J all show negative alongshore shear, indicating faster winds nearshore and counterclockwise rotation. Confusingly, centers K and L show positive alongshore shear indicating the opposite of centers H, I, and J, although it is noted centers J and L have large confidence intervals.

Phase 3 DKPs along the Santa Cruz coastline underscore how much the coastline plays a role in the wind flow (Figure 20). All average vorticity centers along the coast are positive, with max values around Steamers Lane and the smallest values in the Santa Cruz harbor. Positive values indicate that coastal drag from the cliffs located along this coastline influences flow dynamics and helps to turn the wind northward around Steamers Lane. The

normalized Okubo Weiss parameter indicates how shear and stretch play a greater role in the creation of vorticity than rotational vorticity when generating the spin of the air parcel.

Phase 3 canonical day alongshore DKPs of vorticity and shear display similar results throughout the day (Figures 21 and 22). Increased vorticity and shear are observed dwarfing the effects of Coriolis on the air parcel during the peak velocity from the LSB, showing that with increased alongshore winds' rotational effects become more apparent.

D. LARGE SCALE THOUGHTS

The backing of winds with decreasing distance to shore seen within southern Monterey Bay at almost all hours is postulated to be due to the presence of land and the differential roughness influencing wind speed, along with spatial and temporal differential thermodynamic effects from nonuniform heating of the land. One hypothesis pertaining to offshore winds speed behavior postulates that wind speeds and direction would remain constant with decreasing distance to shore, changing once over land due to increased friction slowing the air and decreasing Coriolis forcing, allowing the winds to back (Roeloffzen et al. 1985). Results in this study indicate that while wind speed is relatively constant offshore, wind directions change before flowing over land and encountering increased friction. Furthermore, the increased heating of Salinas Valley and Watsonville region, areas containing many farms compared to other hilly and mountainous areas surrounding Monterey Bay, is a potential cause of why winds within southern Monterey Bay bend northward instead of southward. At night, the pressure gradient sets up between Monterey and Santa Cruz and wind backing continues.

The spatial and temporal wind backing and veering at China Rock are influenced by the synoptic winds, and when the central Monterey Bay LSB forcing is strong. Additionally, coastal topography disrupts wind flow around the peninsula forcing low-level winds to diverge and bend north or south.

Winds along the Santa Cruz coastline are influenced both by the northwesterly synoptic winds and the Monterey Bay LSB, which together increase wind velocity during the afternoon and evening. This increased wind speed increases the DKPs observed along the coastline. Additionally, as winds lose their spatial and frictional cliff constraint of the

coastline east of Steamers Lane in Santa Cruz harbor, winds fan out, turn north, and more easily flow onshore due to coastal topography transitioning into beaches.

E. SOURCES OF ERRORS

Several sources of error can be found within the findings of this paper. Inevitable gaps occurred in the buoy data. Care was taken to filter out bad data that could potentially skew results. DKP calculations assume a linear wind field between buoys, which is not necessarily true with a low viscosity fluid, such as air, when flowing near land or when land lies between buoys. Additionally, all data were collected during the summer months of June-August, meaning synoptic flow patterns for other times of the year are not necessarily reflected in the results discussed in this paper.

THIS PAGE INTENTIONALLY LEFT BLANK

V. SUMMARY

A three-phase experiment was conducted using 46 spar buoys in and around Monterey Bay during June-August 2021 and August 2022. The buoys were outfitted with GPS tracking systems to obtain location data and sonic anemometers at 4m heights to acquire 30-minute averaged wind speed eastings and northings every hour.

Cross and alongshore buoy arrays were used to analyze wind flow patterns primarily influenced by northwesterly synoptic winds and a diurnal sea breeze. Canonical day winds of the cross and alongshore buoy arrays reveal spatial and temporal backing of winds throughout an average day within Monterey Bay due the presence of land and coastal differential roughness influencing wind speed. Across-shore spatial wind backing starting 6.5km offshore of Marina in southern Monterey Bay ranges between 15 to 55 degrees depending on the time of day. This change in wind direction occurs before a change in wind speed has taken place. An analysis of the alongshore canonical day wind flow around the Monterey Peninsula and Santa Cruz illustrates how friction and flow disruption by coastal topography affects coastal wind dynamics by decreasing wind speed nearshore and causing spreading of cross-shore wind vectors.

The response to wind veering and backing that induce cross-shore and alongshore spatial gradients in the wind can be described and quantified with DKPs. DKPs were calculated at triangle center points each hour using buoy locations as triangle corners. Average vorticity and normalized Okubo Weiss illustrate how rotational vorticity plays a minor role compared to shear within the coastal environment. Additionally, canonical day vorticity and shear illustrate the LSB influence on wind flow dynamics with DKP maximums occurring during peak LSB forcing.

THIS PAGE INTENTIONALLY LEFT BLANK

LIST OF REFERENCES

Abbs, D. J., Physick, W. L., 1992: Sea-breeze observations and modeling: a review. *Aust. Meteorol. Mag.*, **41**: 7–19.

Archer, C. L., Jacobson, M. Z., 2005: The Santa Cruz Eddy. Part II: Mechanisms of Formation. *Mon. Wea. Rev.*, **133**, pp. 2387–2405.

Banta, R. M., Oliver, L. D., Levinson D. H., 1993: Evolution of the Monterey Bay S ea-Breeze As Observed by Pulsed Doppler Lidar. *J. Atmos. Sci.*, **50**: 24, pp. 3959–3982.

Brettle, M. J.,1994: An investigation of possible systematic wind-direction changes associated with sudden increases in wind speed. *Met Apps*, **1**: pp. 179–183.

Darby, L. S., Banta, R. M., 2002: Comparisons between Mesoscale Model Terrain Sensitivity Studies and Doppler Lidar Measurements of the Sea Breeze at Monterey Bay. *Mon. Wea. Rev.*, **130**: pp. 2813–2838.

Davies-Jones, R., 1992: Useful Formulas for Computing Divergence, Vorticity, and Their Errors From 3 or More Stations. *Mon. Wea. Rev.*, **121**, 3, pp. 713–725, https://doi.org/10.1175/1520-0493(1993)121<0713:UFFCDV>2.0.CO;2.

Dukhovskoy, D. S., Bourassa, M. A., Petersen, G. N., Steffen J., 2017: Comparison of the ocean surface vector winds from atmospheric reanalysis and scatterometer-based wind products over the Nordic Seas and the northern North Atlantic and their application for ocean modeling. *Journal of Geophysical Research: Oceans*, **122**, 1943–1973, https://doi.org/10.1002/2016JC012453.

Gao, Q., Zeman, C., Vergara-Temprado, J., Lima, D. C. A., Molnar, P., Schär, C., 2022: Vortex streets to the lee of Madeira in a km-resolution regional climate model. *EGUShpere*, pp. 1–34, https://doi.org/10.5194/egusphere-2022-965.

Henrickson, J., MacMahan, J., 2009: Diurnal sea breeze effects on inner-shelf cross-shore exchange. *Continental Shelf Research*, **29**: pp. 2195–2206, https://doi.org/ 10.1016/j.csr.2009.08.011.

Kovatch, M., Feddersen, F., Grimes, D. J., MacMahan, J. H., 2021: Vorticity Recirculation and Asymmetric Generation at a Small Headland With Broadband Currents. *Journal of Geophysical Research: Oceans*, **126**, pp. 1–24, https://doi.org/10.1029/2020JC016639.

Kudryavtsev, V. N., Makin, V. K., Klein Tank, A. M. G., and Verkaik, J. W., 2000: A model of wind transformation over water–land surfaces. *KNMI Scientific Report*, WR-2000-01, KNMI, De Bilt, The Netherlands, pp. 1–30.

Mestayer, P. G., Calmet, I., Herlédant, O., Barré, S., Piquet, T., Rosant, J., 2018: A Coastal Bay Summer Breeze Study, Part 1: Results of the Quiberon 2006 Experimental Campaign. *Boundary-Layer Meteor.*, **167**, pp. 1–26, https://doi.org/10.1007/s10546-017-0314-6.

Miller, S. T. K., Keim, B. D., Talbot, R. W., Mao, H., 2003: Sea breeze: Structure, forecasting and impacts. *Rev. Geophys.*, **41**: 1011–1042.

Ohlmann, J. C., Molemaker, M. J., Baschek, B., Holt, B., Marmorino, G., Smith, G., 2017: Drifter observations of submesoscale flow kinematics in the coastal ocean. *Geophys. Res. Lett.*, **44**, 3, pp. 30–337, doi:10.1002/2016GL071537.

Pullen, J., Caldeira, R., Doyle, R. D., May, P., Tome, R., 2017: Modeling the air-sea feedback system of Madeira Island. *Journal of Advances in Modeling Earth Systems*, **9**, pp. 1–24, https://doi.org/10.1002/2016MS000861.

Roeloffzen, J. C., Van Den Berg, W. D., Oerlemans, J., 1985: Frictional Convergence at Coastlines. *Tellus*, **38A**: pp. 397–411.

Rudnick, D. L., Zeiden, K. L., Ou, C. Y., Shaun Johnston, T. M., MacKinnon, J. A., Alford, M. H., Voet, G., 2019: Understanding Vorticity Caused By Flow Passing an Island. *Oceanography*, **32**, 4, 66–73, https://doi.org/10.5670/oceanog.2019.410.

Savijärvi, H., 2004: Model predictions of coastal winds in a small scale. *Tellus*, **56A**: pp. 287–295.

Smith, R. B., Gleason, A. C., Gluhosky, P. A., 1997: The Wake of St. Vincent. *J. Atmos. Sci.*, 54, pp. 606–623.

Steele, C. J., Dorling, S. R., von Glasow, R., Bacon, J., 2014: Modelling sea-breeze climatologies and interactions on coasts in the southern North Sea: implications for offshore wind energy. *Quarterly Journal Review of the Meteorological Society*, **141**: pp. 1821–1835, https://doi.org/10.1002/qj.2484.

Tseng, Y. H., Chien, S. H., Jim, J., Miller, N. L., 2011: Modeling Air–Land–Sea Interactions Using the Integrated Regional Model System in Monterey Bay, California. *Mon. Wea. Rev.*, **140**: pp. 1285–1306, https://doi.org/10.1175/MWR-D-10-05071.1.

Woodson C. B., Eerkes-Medrano. D. I., Flores-Morales, A., Foley, M. M., Henkel, S. K., Hessing-Lewis, M., Jacinto, D. et al., 2007: Local diurnal upwelling driven by sea breezes in northern Monterey Bay. *Continental Shelf Research*, **27**: pp. 2289–2302, https://doi.org/10.1016/j.csr.2007.05.014.

INITIAL DISTRIBUTION LIST

1. Defense Technical Information Center
   Ft. Belvoir, Virginia

2. Dudley Knox Library
   Naval Postgraduate School
   Monterey, California